Manuscript prepared for J. Name
with version 5.0 of the LaTeX class copernicus.cls.
Date: 16 December 2014

Analysis of the ozone profile specifications in the WRF-ARW model and their impact on the simulation of direct solar radiation: Revised version

A. Montornès[1,2], **B. Codina**[1], **and J. W. Zack**[3]

[1]Department of Astronomy and Meteorology, University of Barcelona, Barcelona, Spain
[2]Information Services, AWS Truepower, Barcelona, Spain
[3]MESO Inc., Troy, USA

Correspondence to: A. Montornès (amontornes@am.ub.es)

This document provides a detailed point-by-point response to all referee comments and specifies all changes on the revised manuscript.

First of all, we would like to express thanks for the suggestions, comments and ideas provided by our Editor and both referees.

The paper entitled *Analysis of the ozone profile specifications in the WRF-ARW model and their impact on the simulation of direct solar radiation* was published in the Atmospheric Chemistry and Physics Discussion in 6^{th} August 2014. During the Open Discussion period, the paper was reviewed by two anonymous referees.

The first review was received in 29^{th} August 2014 by the Anonymous Referee #2 while the second one was published in 3^{rd} August 2014 by the Anonymous Referee #1.

In 12^{th} November 2014, we submitted two documents as a response to referees reviews: Response to "Reviewer Comments", Anonymous Referee #1 and Response to "Referee Comment for ACP Manuscript acp-2014-143", Anonymous Referee #2.

With this document, we submit the revised version of the paper based on the aforementioned responses. The document is divided in four blocks. The first one is composed of these paragraphs. Through each one, we will explain the structure and we will define the used nomenclature that will be useful for the next sections.

The following three sections show all the responses again. The idea is to make easier the revision of the changes. In general, the text is the same that the submitted in 12^{th} November 2014. However, some parts have been updated after the revision and others have been summarized.

Some points are common for both referees or they have a full impact to the entire paper. For this reason, we will present firstly a common block and then we will discuss each review point by point. Hereinafter, we will use R#1 and R#2 such as Referee #1 and #2, respectively.

In order to contextualize the response, the referee's commentary appears before our answer. Each review is quoted in gray. Our response appears with **A:** (from Authors) at the beginning and in black color. Each one is identified with a label composed with a number and a tag: GC (General Comments) and SC (Specific Comments). For example, SC4 refers to the 4^{th} specific comment. During the discussion, the reader can find some cross-references between responses for R#1 and R#2. For example, **SC7 R#1** means the 7^{th} specific comment of R#1.

Some of the answers are also aimed to the Editor. These responses are: **GC4 R#1**, **SC4 R#1**, **SC8 R#1**, **GC4 R#2**, **SC10 R#2** and **SC67 R#2**.

The last part of the document refers to the new version of the article. The old text appears in red and crossed out while the new parts are typed in blue and underline. The parts in black indicate the same text for both versions. In order to compare easier the document changes and the responses, the label of each response (e.g. **SC14 R#2**) appears always before the modification. The R#1 and R#2 are colorized in brown and green, respectively.

Nevertheless, these rules require some exceptions. As it was detailed in **GC1 R#2**, some parts of the paper needed to a better explanation and contextualization. Moreover, **SC10 R#1** and **GC3 R#2** suggested that the paper needed careful proof-reading for English grammar and style. This new version tries to improve these points. In order to avoid a tedious

document, some changes are well indicated in color, but they are not labeled.

One important modification in the paper has been the units of the results (see the Common comments and **SC8 R#1**). As a consequence, we have introduced many changes in section 3. These changes are colorized but they are not labeled.

1 Common comments

By our understanding, both referees agree that the first part is interesting but they have doubts regarding if the second one was addressed correctly. Nevertheless, they diverge on the reasons and the solutions about that. In short, R#1's opinion is that we are analyzing the absorption instead of the direct flux whereas R#2's perspective is that a full WRF simulation (at the least for one time step) could address better the discussion.

A further discussion about these considerations is presented in the following points: **GC1 R#1**, **SC7 R#1**, **SC8 R#1**, **GC1 R#2** and **SC35 R#2**.

Introduction

We have concluded that we can improve the introduction in two aspects: i) a better contextualization of the interest of the paper and ii) a better explanation of the presented ideas.

Further information is presented in **SC4 R#2** and **GC1 R#1**.

Methodology

Based on the ideas from both referees, we propose a set of updates in the methodology in order to increase the scientific significance of the results. Two of them have an important impact in the paper structure and the others introduce small improvements or clarifications in the current text. Through the following paragraphs, we will present a small overview of these modifications. You can find further details in the full text at the particular responses (referred in the following explanation).

In his review, R#2 suggested that excluding the GFDL scheme from the analysis deprives the readers from the opportunity to understand its accuracy relative to the other methods (see **SC12 R#2**). We agree about this consideration and we have decided to add this parameterization to the discussion, thus giving a global vision of WRF. As a consequence, we propose to add some changes on section 2 (providing further details about this parameterization), on sections 3 and 4 (adding this scheme to the discussion) and on the figures (adding the respective maps).

On the other hand, from the commentaries of R#1 (see **GC1 R#1** and **GC2 R#1**), we have concluded that we could show and discuss the vertical profiles provided by each scheme. Moreover, this discussion could be linked with the current results and conclusions. As we understand it, this small study could be interesting to the scientific community as well as for the WRF users because it is missing in the state-of-the-art.

Results

After reading the review from R#1, we have concluded that the used metrics are useless for a good paper understanding (see **GC4 R#1** and **SC8 R#1**). We would like to improve this point.

In the first part (sections 2.2 and 3.1), our discussion was based on the relative error (equation 5 in the paper) without including any figure as a baseline (e.g. monthly maps for the MSR data-sets). We concluded that this way of showing the results is useless if the reader does not have a background about the ozone spatial and seasonal distributions. In order to correct this point, without adding new figures, we propose to replace the relative error by the bias (in Dobsons). As a consequence, equation 5 in the paper, section 3.1, Conclusions and Figures 1 and 2 must be updated accordingly.

In the second part (sections 2.3 and 3.2), we computed the bias in the ozone absorption (equation 22 in the paper) normalized with respect to the radiation at the top of the atmosphere. As a result, we compared two percentages and we lost the physical sense of the results. To improve this point, we propose to show the results as W m^{-2} multiplying the previous results by the incoming radiation at the top of the atmosphere. Sections 2.3 and 3.2, Conclusions and Figure 3 must be updated accordingly.

Figures

Both referees noted that the quality of the images could be improved. We agree about these considerations. The original figures were created using the R language. We have been testing the NCAR Command Language and it clearly improves the quality of the results.

2 Response to "Reviewer Comments", Anonymous Referee #1

Response to general comments

GC1 R#1: In this paper, the authors aim at analyzing i) the ozone representation in the shortwave (SW) radiative transfer schemes of WRF, and ii) the impact of the biases in this representation on the predicted direct solar radiation. Three different ozone representations have been analyzed: one which is shared by the Goddard, New-Goddard and Fu-Gu-Liou SW schemes, and two more used in the CAM and RRTMG SW schemes, respectively. The two objectives are clearly set out at the beginning of the paper but, to my view, the interest of the study is not sufficiently well motivated.

The methods used are appropriate to achieve the proposed objectives. However, I have concerns regarding how the second objective was addressed. In my opinion, the interest of the paper has not been clearly set out. This work deals with stratospheric ozone. Thus, in principle, it has high interest for WRF's applications in the stratosphere. However, only total ozone has been verified and nothing is said regarding how the vertical profile of ozone is represented in WRF. This limits the interest of the study for "stratospheric" applications. In any case, authors should add comments on how important is a correct vertical distribution for the vertical distribution of heating rate, and the coincidences and differences in this with respect in the analyzed data bases. It is claimed that this study has interest for solar energy, more specifically, for solar energy forecasting. However, in my opinion, this importance should be better contextualized.

A: Regarding to the second objective issue, we will provide a full explanation about the ideas and procedures to address in the **GC1 R#2** response. In the following lines, we will focus our discussion on your commentaries about the stratosphere and the solar energy forecasting.

We agree that the work deals with stratospheric ozone. However, it also deals with solar modeling. In its travel throughout the atmosphere, a solar beam is absorbed and scattered by atmospheric gases (e.g. water vapor, ozone) and particles (e.g. aerosols, cloud droplets). Therefore, to compute the solar radiation reaching the surface is requires understanding all these physical processes that occur in the atmosphere.

In a clear sky atmosphere, basically two gases absorb the solar radiation: water vapor and ozone. In the troposphere, water vapor absorbs solar radiation in some near-infrared (near-IR) spectral bands.

On the other hand, ozone is located in two atmospheric regions with a different impact on the radiative transfer. Most ozone ($\sim$90%) is located in the stratosphere while the remaining ozone ($\sim$10%) is found in the troposphere. The stratospheric ozone absorbs solar energy in a few bands of ultraviolet (UV) and photosynthetic active region (PAR) whereas the impact of the tropospheric ozone on the radiative transfer is negligible.

Hence, all approximations assumed on modeling these contributions have an impact on the accuracy. Of course, other elements such as aerosols or clouds have a higher impact and, at the same time, they are more difficult to be improved. In contrast, as we presented in the paper, ozone introduces smaller errors that, moreover, could be easily reduced. From our perspective, an understanding of the physical processes is significant *per se*, beyond the impact on the output accuracy.

When we started to work on this study, we were worried because the lack of literature analyzing the impact of the ozone modeling on radiative codes and we decided to introduce a scientific discussion about that. In the first part, we presented a detailed information of the ozone treatment in the radiative parameterizations of the WRF-ARW that we considered that could be of interest to many WRF-ARW users and solar modeling researchers.

In addition to this, the shortwave radiation absorbed by ozone in the stratosphere is the primary physical process in maintaining its thermal structure. Thus, the stratosphere is a parallel topic but it is not the focus of the analysis. Nevertheless, from your considerations, we recognize that the paper can be enhanced if we introduce more details about the stratosphere on the discussion.

A validation of the vertical profiles is not feasible under the structure of the presented work because a global and climatic ozone profile dataset with a reasonable horizontal resolution does not exist. The ozone-soundings are provided generally from balloon and aircraft campaigns at several sites and for limited periods. Furthermore, many of these sites are located in the United States. We searched this kind of data in the NOAA Earth System Research Laboratory server (ESRL), the Climate Prediction Center (CPC) and the National Climatic Data Center (NCDC) without success.

In contrast, satellite data provide global and climate measurements with good spatial resolution. However, these data are vertically integrated such as in the Total Ozone Mapping Spectrometer (TOMS) Data or the MSR used in the present analysis. For this reason, we decided to use the MSR dataset as a baseline for our analysis.

In order to include your ideas, we propose the following improvements:

- A better contextualization of the paper in the introduction following the aforementioned ideas.
- Add new figures plotting the ozone profiles for each scheme and a description in section 2.1.
- Link the discussion of the results to those figures.

Moreover, we consider that this type of figures can increase the scientific significance of the paper because similar plots do not exist in the state-of-the-art.

GC2 R#1: I miss some comments on the average absorption due to ozone in typical conditions, so that the reader receives a clearer message on the importance of ozone for solar energy.
Since it is claimed that "high spatial and temporal variability" of ozone occurs in the stratosphere, it would be helpful if some figures were given of the expected range of seasonal variability in a point and spatial variability for a fixed season and how they translate to solar radiation extinction. These simple numbers would help to advance the reader the order of magnitude of the corrections that could be achieved with an improved representation of ozone. This could be compared with the typical errors of WRF in solar energy forecasting applications.

A: The response to these considerations is linked to the previous one. The new figures related to the ozone profiles can be useful for the reader to understand the order of magnitude of the ozone variability.

In addition, we agree about the idea of including some numbers to help the reader to understand the paper.

Finally, as we detail in **SC8 R#1**, we propose to show the bias in W m^{-2} instead of percentages. This improvement will be useful in order to clarify some ideas.

GC3 R#1: One application that is not even mentioned is the modeling of shortwave irradiance in the UV part of the spectrum. The SW schemes analyzed make spectral computations. Could have been this analyzed somehow? Moreover, the latest WRF versions provide broadband direct and diffuse irradiance with RRTMG and New-Goddard. Could they be used to investigate the impact of ozone misrepresentation on irradiance fluxes?

A: Regarding the application for modeling of shortwave irradiance in the UV part of the spectrum, we agree with the reviewer that it is important from the point of view of the radiative transfer models. Nevertheless, we did not mention this application because this is not the "natural" usage of solar parameterizations in mesoscale NWP models and particularly, in WRF.

In general, the shortwave schemes in WRF divide the spectrum in a few bands (from 1 in Dudhia's case to 8-16 in the other schemes). Upward and downward fluxes are computed at each band in terms of different contributions. Some contributions are specific of that band (e.g. ozone in the UV or water vapor in the near-IR) and others are general for all of them (e.g. clouds or aerosols). The total upward and downward fluxes are the sum over all the bands (i.e. spectral integration). In order to reduce computational memory, the intermediate values are generally stored in temporal arrays that are removed at each computation step.

Moreover, note that the shortwave schemes in the model are not designed for spectral applications. In the past, the shortwave schemes were necessary to set the day-night behavior on NWP simulations. Therefore, the greatest interest of this kind of parameterizations was the total absorbed energy (i.e. the heating rate) profile and the total global horizontal irradiance at surface for the land model. A full treatment of the radiative problem was computationally expensive (even nowadays). Therefore, the general methodology was to reduce the computational time by reducing the complexity of the methods (e.g. using a few bands instead of line-by-line computations). With this usage of the radiative codes, accuracy was not a matter of concern because other sources of error had a higher impact.

In recent years, the interest for modeling the solar resource by using NWP models has increased and, as a result, also the interest for a good accuracy on global, direct and diffuse irradiances. Nevertheless, the radiative codes are the same as in the past.

Thus, from our perspective, the radiative codes in WRF are not good tools to be used for spectral purposes. There are other external codes more complex that are ready to perform this type of studies.

Setting aside these set of considerations, note that we are actually analyzing the UV and PAR regions. Let us simplify the problem and imagine a scheme with three bands: UV, PAR and near-IR. Since ozone absorption occurs in the UV and PAR bands, we can write the total direct flux as

$$F_{dir}^{sch} = F_{dir,UV}^{sch}(O_3) + F_{dir,PAR}^{sch}(O_3) + F_{dir,nearIR}^{sch}, \quad (1)$$

when we use the scheme ozone data, and

$$F_{dir}^{MSR} = F_{dir,UV}^{MSR}(O_3) + F_{dir,PAR}^{MSR}(O_3) + F_{dir,nearIR}^{MSR}, \quad (2)$$

when we use the MSR dataset.

If we only consider the ozone contribution, then the atmosphere is transparent in the near-IR. Thus, both terms $F_{dir,nearIR}^{sch}$ and $F_{dir,nearIR}^{MSR}$ are mutually canceled when we compute the bias.

Regarding the second question, we agree with the reviewer when he says that the RRTMG and New Goddard parameterizations provide spectrally integrated direct and diffuse irradiance components. However, this is not required as we detailed in **GC1 R#2**.

In short, ozone does not have an explicit contribution on the diffuse component. The molecular scattering is considered in the Rayleigh's term and it assumes dry air mass without considering any kind of species. Therefore, the ozone dataset does not play any role on the scattering computation.

On the other hand, in the computation of the Beer-Lambert law, we can consider each contribution to the optical thickness (e.g. water vapor, ozone, ...) independent one another.

Hence, we can analyze the ozone impact on the direct flux without considering the other elements.

GC4 R#1: To my view, the study of the impact of the ozone misrepresentation on the computed direct irradiance has not been totally addressed. This analysis has been done showing maps and numbers of absorption biases, instead of the expected irradiance biases. However, the irradiance biases can be very easily computed by including the effect of solar geometry. Unless these maps are included in the paper and the results analyzed in terms of irradiance biases I don't agree that this paper addresses the impact of ozone errors on the direct solar irradiance. I would encourage the authors to address these issues and the specific comments detailed below.

A: The radiative schemes use the ozone data to compute the direct flux (see **GC1 R#1**) while the molecular scattering (i.e. diffuse component) of these molecules is considered in the Rayleigh term without any consideration about the gas species. Therefore, since this paper is focused on the ozone profiles, we only validate the direct flux because the diffuse one does not depend on the ozone data.

In a non-scattering medium, when a solar beam travels throughout a layer, one part of the energy is absorbed A by the medium and the other part is transmitted T to the next layer (energy conservation). In other words, if we consider normalized values

$$1 = A + T. \quad (3)$$

Therefore, when we compare the outcomes using the MSR dataset and the ozone data provided by each scheme, the biases on the absorption and transmission are the same but with opposite sign.

As we normalized the results with respect to the radiation at the top of the atmosphere (TOA), we plotted the absorption because it was more understandable. All this information appears in the equations. Furthermore the nomenclature is coherent during all the paper. Thus, from our point of view the ozone misrepresentation on the computed direct irradiance has been well addressed.

In the response at point **SC10 R#1**, we propose to show the results with physical units (i.e. W m^{-2}). Hence, we can plot the direct radiation instead of the absorption if the Editor thinks that it is better. Nevertheless, from our understanding, this type of plots will not add any new information.

GC5 R#1: I would also suggest the authors to use the knowledge acquired in this work to improve the current representation of ozone in WRF (for instance, by including the MSR dataset in WRF and making it available for the SW schemes). WRF is public and freely available for anyone and I am sure that the WRF's community would be thankful.

A: This idea sounds good but is not be feasible with the MSR dataset. The MSR considers the total ozone amount instead of the vertical profiles that are required by the WRF model to compute the heating rate profile at each grid-point (see **GC1 R#1**).

As the dataset provided in CAM shows the best accuracy when it was compared with the MSR data, it could be used for the other schemes.

In fact, from version 3.5 the RRTMG can utilize the ozone profiles available in the CAM scheme with the option o3input in the namelist.input file (as we commented in the paper). This improvement could be added in the other parameterizations with some code modifications.

We will add this suggestion on the Conclusions and we will explore this idea as a future work (see **GC5 R#2**).

Response to specific comments

Title: Analysis of the ozone profile specifications in the WRF-ARW model and their impact on the simulation of direct solar radiation

SC1 R#1: I don't see the title appropriate for a threefold reason:

R#1: i) only the total ozone amount has been analyzed, but not the "ozone profile" (i.e., the vertical distribution of ozone);

A: It is true that we are analyzing the total ozone amount. However, the main idea of the paper is to offer to the scientific community a description about the simplifications that are assumed in the ozone treatment within the radiation options of the WRF model and a quantification of the impact of these assumptions.

In section 2.1 we provide a full description of the ozone datasets that can be improved as we suggest in **GC1 R#1**. In section 2.2, we compute and validate the total ozone amount because 4D (spatial and temporal) ozone datasets are not available (further details in **GC1 R#1**).

Therefore, from our perspective, this part of the title is correct because the ozone profile datasets are the subject at matter in which the study is developed.

R#1: ii) the impact of the ozone misrepresentation is analyzed, and not the impact of the ozone profile "specifications"; and

A: From our point of view, what we have done is analyzing the ozone profile specifications to asses the impact of the ozone misrepresentation. Moreover, as we referred in the previous paragraph, we also provide a full analysis of the profiles in section 2.1 that can be improved after this revision.

R#1: iii) the impact on the solar radiation absorption is analyzed, and not the "impact on the direct solar radiation"

A: We believe that "direct solar radiation" is justified following our discussion in **GC4 R#1** regarding the relationship between absorption and transmission.

Probably the title could be improved but, from our point of view, it is a good representation of the paper's content.

Section 2.1

SC2 R#1: I don't think you have necessarily to distinguish always between the Goddard and New-Goddard SW schemes. The new SW Goddard is essentially the Goddard scheme (Chou and Suarez, 1999) with only few minor modifications (http://www.atmos.umd.edu/∼martini/wrfchem/ppt/WRF_Toshi.ppt). You can mention you are using the new version implemented in WRF and from there on just talk about Goddard SW scheme.

A: We understand your point of view and it is true that New Goddard is an updated version of Goddard. However, we think that is better to distinguish both schemes because:

i) they are different model options (i.e. Goddard was not overwritten by New Goddard). Hence, the paper can be more useful for the WRF's users (see **SC12 R#2**),

ii) the source code of New Goddard was rewritten with many differences at computational level. These code changes lead to significant differences in the applicability. For example, New Goddard can not be coupled to the WRF-CHEM, while Goddard can. Concluding, both assume the same approximations but the differences in the code are significant to be distinguished in the paper.

SC3 R#1: One more thing is that the reference Chou et al. (2001) is not appropriate because it is for the longwave Goddard scheme only.

A: We included this reference in terms of the available literature that is listed in the code of the New Goddard scheme (module_ra_goddard.F).

The code referring to the physical processes in the UV and PAR bands is based on Chou et. al. (1999), while the code referred to the near-IR is based on Chou et. al (2001). Therefore, we chose both references as relevant to the scheme.

Since the WRF-ARW User's Guide lists the primary references of each parameterization, we have decided to follow that nomenclature to avoid misunderstandings on the readers. A complementary explanation is given in **SC13 R#2**.

SC4 R#1: Could you provide details and/or references on the origin of the ozone profiles used in each SW scheme?

A: Sorry, we can not. We tried to search this information when we wrote the paper, but without success. In general, this information does not appear on the source code or in the based papers. Finally, we decided that this information was not mandatory for the paper. However, we could try to contact the authors to ask them if the Editor thinks that it could be valuable to enhance the paper.

SC5 R#1: I don't understand: "The RRTMG scheme includes two ozone profiles as a function of the season (winter and summer). Nevertheless, this granularity is useless due to the fact that the final used profile is computed as a composition of both, without considering the day of the year. Therefore, only one profile is considered for any latitude and season." Could you please explain better? Why is it useless? Is it not used in RRTMG?

A: As we summarized in Table 1, the ozone data of this parameterization is stored in a subroutine O3DATA located in a file denoted module_ra_rrtmg_lw.F (note that the letters *lw* are not a mistake).

Given one grid-point, this routine has three inputs: the pressure at the relative ETA levels of that point, the starting index for the vertical levels (in all the cases, 1) and the ending index for the vertical levels (in all cases, the number of vertical levels). In order to reduce the discussion, we will disregard the difference between full and half levels.

As output, this routine returns the ozone profile interpolated to the ETA levels.

When you begin to read the code, you find 4 arrays with a dimension of 31 elements each one: O3SUM, O3WIN, PPSUM and PPWIN where O3 denote the ozone mixing ratio (kg/kg), PP the pressure (hPa), SUM summer and WIN winter.

These arrays store two ozone profiles: one for summer and one for winter.

In the next step, two new arrays are built: PPANN and O3ANN, both with a dimension of 31 elements.

In the PPANN is stored the PPSUM array (this process is completely arbitrary).

Given one element K, the O3ANN(K) is computed as

```
O3ANN(K)=O3WIN(K-1)+(O3WIN(K)-O3WIN(K-1))/
         (PPSUM(K)-PPWIN(K-1))
O3ANN(K)=0.5*(O3ANN(K)+O3SUM(K))
```

Finally, this array is interpolated to the ETA levels and returned to the main code flow.

You can note that, although this scheme contains two ozone profiles, this information is not actually used. As a result, we have a single profile that is invariant on latitude and time.

When we prepared that paper, we decided to summarize this information because we believed it was not important for the purpose of this study. The key point it is that this parameterization only uses one scheme. As we indicated in the paper, this scheme can work with the CAM dataset but we chose the original settings.

The paragraph has been reworded to be more clear.

Section 2.2

SC6 R#1: How did you re-grid the datasets to 1 deg x 1 deg ?

A: As both MSR and ERA-Interim are defined in a regular lat-lon grid, we used a simple bi-lineal interpolation.

Section 3

SC7 R#1: Why can you validate the RRTMG's ozone amount but not the impact of its misrepresentation on direct solar irradiance? Why do you only validate the impact using the Goddard and CAM ozones? I don't understand this point.

A: We can validate the RRTMG's ozone amount because we can isolate the vertical profile (see **SC5 R#1**) and integrate vertically from the surface to the top.

In contrast, we can not validate the impact of its misrepresentation on direct solar irradiance as we will argue in the following lines.

From equation 20 (in the paper), we know that the absorption can be computed as

$$A(\tau/\mu_0) = 1 - \int_0^\infty W(\lambda) e^{-\tau_\lambda/\mu_0} \mathrm{d}\lambda \tag{4}$$

where the optical thickness τ_λ from the TOA to a level z may be expressed as

$$\tau_\lambda(z) = \int_z^\infty k_\lambda \rho q_{O_3} \mathrm{d}z, \tag{5}$$

where k_λ denotes the mass absorption cross section and ρ is the dry air density.

This integral requires the vertical information of the ozone mixing ratio and the dry air density.

The mass absorption cross section is the ability of one molecule to absorb a photon given a particular wavelength. Nevertheless, in the atmosphere, the molecules are not isolated and they interact the ones with the others. As a consequence, monochromatic absorption is rarely observed because the energy levels during energy transitions are changed due to the external influences. Therefore, the radiation absorbed during consecutive energy transition is non-monochromatic and the spectral lines are broadened.

In virtue of the kinetic theory of gases, the dependence of the k_λ on temperature and pressure can be demonstrated. Hence, as τ_λ is a function of the height and this is a function of the temperature and pressure, the integral can not be computed without a detailed information about k_λ.

Regarding the spectral integration, the best method to compute equation 4 is the line-by-line (LBL) calculation. However, this method is not computationally feasible because would require many thousands of computations at each grid-point. Instead of this, some approximations are assumed in terms of the gas and its spectral behavior. For example, the water vapor absorption has a high variation with the wavelength and the K-distribution method is required (see Liou (1980)).

Other gases as the ozone show a lower variation with the wavelength and an effective k_λ is used for each spectral band. This coefficient is previously computed using the LBL at a reference value of pressure and temperature. Finally, this value is scaled to the pressure and temperature of each layer in order to consider the dependency on these magnitudes.

In WRF, New Goddard and CAM use this second approximation while the RRTMG uses the K-distribution method.

Moreover, the dependency of the ozone absorption with pressure and temperature is small and New Goddard and CAM do not scale this magnitude (see, for example, Chou and Suarez(1999)).

Therefore, in New Goddard and CAM, k_λ can be assumed as a constant with height and τ_λ is

$$\tau_\lambda(z) = k_\lambda \int_z^\infty \rho q_{O_3} \mathrm{d}z, \tag{6}$$

or using the hydrostatic equation and considering the entire atmosphere

$$\tau_\lambda(p_\mathrm{s}) = \frac{k_\lambda}{g} \int_0^{p_\mathrm{s}} q_{O_3} \mathrm{d}p. \tag{7}$$

The integral is directly the ozone amount described by equation 3 (in the paper). Therefore, we can evaluate the radiative absorption without any information about the vertical distribution.

In contrast, the RRTMG considers the dependence of k_λ on height and we need to know the vertical structure of the atmosphere to solve τ_λ.

Since the vertical profile from the MSR dataset is not available, we can not compute this integral for the baseline dataset. For this reason, we did not include the analysis of the RRTMG scheme.

Results

SC8 R#1: It would be interesting to add annual results, not only monthly. As mentioned earlier, direct solar irradiance biases (in W m^{-2}, and in % would be also interesting) should be shown instead of absorption biases.

A: We think that, the annual results are a good way to summarize the results but they do not contribute with new information since ozone shows a well-defined seasonal pattern. Then, in our opinion, it is not necessary.

Regarding the direct solar irradiances, we agree about your consideration. We propose to update all the figures to show the results in W m^{-2}. This update involves some modifications in the Methodology (section 2.3) and in the Results discussion (section 3.2).

Figures and Tables

SC9 R#1: Split both Fig. 1 and Fig. 3 in two figures.

A: We agree about this point. We will wait until the Editor's decision.

Others

SC10 R#1: Technical Corrections Needs careful proofreading for English grammar and style.

A: We have tried to address and to improve this point.

3 Response to "Referee Comment for ACP Manuscript acp-2014-143", Anonymous Referee #2

Response to general comments

GC1 R#2: This paper describes the specification of ozone profiles used within most of the WRF-ARW radiation options, compares these to the MSR total ozone dataset, and reviews the impact of the differing ozone amounts on the calculation of the direct solar radiation in two of the WRF radiation options. The first part of the analysis, which compares the various WRF ozone specifications to the MSR data, is a very useful demonstration of the degree to which the ozone concentrations vary spatially and temporally among the radiation codes. While the worthwhile goal of the second part of the analysis is to illustrate the isolated impact of the ozone differences using a consistent, if simplified, radiative transfer method, this result does not relate directly to how the ozone variations contribute to actual radiation calculations within WRF. The paper would be more useful to the WRF user community if the authors added an analysis using one or more of the WRF radiation codes so that the full complexity of the radiative processes involved were represented. For example, the two models applied in the second part could be run within WRF for a single time step for some region or globally. In different experiments, each radiation code could be run with its own ozone specification and then run again with the ozone concentration from the other radiation code. This might be an insightful way to demonstrate the impact of the ozone changes within the context of actual WRF calculations.

A: As we understand it, full WRF simulations are not necessary in the second part of the paper (this answer links with point **SC35 R#2**). We will argue this idea through the following lines.

The general approach in all the radiative codes is to assume independent columns at each grid-point. In brief, the upward and downward solar fluxes are solved at each column considering the vertical profile information provided by the model (e.g. air density, water vapor or hydrometeors) and a set of auxiliary information that is not explicitly solved by the NWP model such as the ozone or the other trace gases (e.g. oxygen, carbon dioxide). Forgetting Dudhia's parameterization that is a special case, the downward component is split in two contributions: direct and diffuse. The first component is solved by using the Beer-Lambert law, while the diffuse contribution requires solving the radiative transfer equation (RTE) assuming different approximations.

Given one wavelength interval, two variables are necessary to solve the Beer-Lambert law: the optical thickness and the cosine of the solar zenith angle. The first one is a function of the absorption/extinction coefficient (intrinsic magnitude of the material) and the mass amount traversed by the solar beam. The second one is a result of positional astronomy.

The RTE is solved in terms of the same variables, the single scattering albedo and the asymmetry factor. Both last describe how the light is scattered.

In the atmosphere, there are many elements that contribute to the absorption and the scattering processes (e.g. ozone and water vapor absorption or the molecular scattering among others). Thus, the total optical thickness, τ_t, the total single scattering albedo, ω_{0t}, and the total asymmetry factor, g_t, are a function of those contributions.

As a first order approximation (widely used in the radiative codes), we can assume that all these contributions are independent one another. Following this assumption, the radiative variables may be split as the sum of contributions as

$$\tau_t = \sum^{N} \tau_i, \tag{8}$$

$$\omega_{0t} = \sum^{N} \omega_{0i}, \tag{9}$$

$$g_t = \sum^{N} g_i, \tag{10}$$

where N is the number of elements (e.g. ozone, aerosols, ice crystals, molecular scattering, water vapor, etc).

In virtue of the exponential form of the Beer-Lambert law, the total transmission of the direct beam through a layer is the product of each contribution. Thus, each one of them can be analyzed independently and we can consider the ozone impact without the other elements.

Regarding the diffuse component in the ozone's case, the radiative parameterizations do not consider explicitly this gas as an scatter element (i.e. ω_{O3} = 0 and g_{O3}=1). The molecular scattering of ozone molecules is parameterized in the Rayleigh scattering term without any differentiation of the gas species. Therefore, the ozone profile is useless in that computation and it can be omitted for the purposes of this paper.

The idea of this reviewer related on real WRF simulations is interesting but the analysis of the problem becomes more complex. In a real simulation, new sources of error are overlapped due to the number of vertical levels, the distribution of the ETA levels and the top of the model. Vertical ozone profiles are interpolated to the domain's ETA levels, thus the ozone information can be smoothed of even lost. Moreover, the radiative codes approximate the atmosphere composition between the top of the model and the top of the atmosphere (TOA) losing the details in those layers.

Moreover, real simulations add a part of particularism (region, domain settings, etc) that was not desired in our work.

Although the regional particularism could be solved using global simulations (see **SC35 R#2**), this part of the code is not commonly-used and it must be used with caution as it is indicated in the User's Guide:

> Note: since this is not a commonly-used configuration in the model, use it with caution. Not all physics and diffusion options have been tested with it, and some options may not work well with polar filters. Also, positive-definite and monotonic advection options do not work with polar filters in a global run because polar filters can generate negative values of scalars. This implies, too, that WRF-Chem cannot be run with positive-definite and monotonic options in a global WRF setup.

Therefore, we think that the derived conclusions could be useless for the scientific community because we could not be sure about the output reliability.

Concluding, we believe that the proposed methodology is valid because

- We reduce a complex problem in a simpler one based on well supported physics.
- The ozone absorption is independent of the other physical processes.
- We are rigorous and transparent in the derivation of the equations.
- The results are useful as a baseline to quantify the impact of the ozone profile simplifications on the direct flux computation.
- The results and conclusions are general.

However, as a self-criticism this part of the paper should be better explained and contextualized.

GC2 R#2: Furthermore, from this reviewer's perspective, the differing specification of trace gas amounts within each radiation option is a fundamental flaw in the design of WRF-ARW itself rather than the radiation codes. These quantities should be provided to each radiation option in a consistent and sufficiently detailed manner from the host model, rather than be defined haphazardly as presently done. In some cases the radiation codes were extracted from other global models, which define their own ozone specification, while in other cases the radiation codes were provided for WRF independently of any existing dynamical model and without a predefined ozone specification. The authors are encouraged to consider addressing this perspective by using this paper not simply to compare the various ozone approaches but to provide guidance to the community on a better way forward; that is, to provide evidence for the advantages of improving WRF by adopting a unified and accurate approach to atmospheric specification for all of the radiation options.

A: We agree about these ideas. When somebody start to work with the source code, the first difficulties appear. The most relevant is in the nomenclature. In general, each scheme uses a different nomenclature to refer to the same physical

magnitudes (e.g. temperature, pressure, height, ozone, absorption coefficient, etc). As a consequence, the time to work with the codes increases because each one requires starting from zero.

Linked with this, another incoherence is in the physical constants. All these magnitudes are defined in the module share/module_model_constants.F. Nevertheless, these variables are redefined with other names in each code.

Moreover, some processes are similar for all the schemes (e.g. prepare the vertical profiles). All of the common processes could be shared using new subroutines or they could be run in the module_radiation_driver.F and shared as input arguments.

Furthermore, there are more physical differences similar to the ozone profile. For example, the carbon dioxide concentration.

In our opinion, this makes more difficult read the source code and it increases the sources of bugs. However, we understand that it is difficult to deal with the code structure and with the outside contributions.

We will put an emphasis on these issues.

GC3 R#2: From a technical writing standpoint, the manuscript contains numerous grammatical difficulties and unclear sentences that are specified in the detailed comments along with suggested improvements.

A: We have improved all those issues.

GC4 R#2: It is also suggested that the current three figures be separated into five figures. It is recommended that publication of the paper be reconsidered after major revisions to the manuscript are completed.

A: We agree with the point of view of this referee. However, we will wait for the Editor's decision. This response is linked to points **SC67 R#2**, **SC68 R#2** and **SC9 R#1**.

Response to specific comments

Abstract

SC1 R#2: Page 20232, Line 12: The phrase "ozone modeling" suggests a more sophisticated approach than what is described in the paper; the phrase "ozone profile" is recommended.

A: We agree that "ozone modeling" is not correct in this context. However, we prefer to use "ozone profile specifications" in this case.

Introduction

SC2 R#2: Page 20232, Line 23: The first sentence of the Introduction uses a somewhat awkward analogy. The shortwave absorption is more the "fuel" than the "engine". A better start may be "The absorption of shortwave radiation by the surface and atmosphere is the primary source of energy that drives the atmospheric system."

A: We agree that the analogy is not suitable and the language was misused. Nevertheless, we do not fully agree with this proposal because it seems that the "absorption of shortwave radiation" is the unique source of energy. This is not really true because both terrestrial and solar radiation have this role.

In the new introduction, this sentence is not necessary and it has been omitted.

SC3 R#2: Page 20233, Line 2: Specify the peak level of ozone heating in the stratosphere. The authors might also specify here the top pressure level required to simulate the stratospheric ozone heating effectively.

SC4 R#2: Page 20233, Line 24: The phrase "defining a region denoted by ozone layer" is unclear and should be reworded.

A: We agree about these considerations and we have concluded that some parts of the introduction are shallow. For this reason, we propose rewording this part.

SC5 R#2: Page 20234, Line 1: Replace "These results. . ." with "This results. . ."

A: We apologize for this grammatical error. This sentence has reworded.

SC6 R#2: Page 20234, Line 6: If the intended meaning of this phrase is ". . .an analysis of the uncertainties associated with the computation of the direct solar radiation" then reword accordingly, otherwise clarify.

A: We agree about this consideration. We have reworded accordingly.

SC7 R#2: Page 20234, Line 14: Replace "error over the direct" with "error on the direct"

A: We have corrected this error.

SC8 R#2: Page 20234, Line 15: Replace "composed only by ozone" with "composed only of ozone"

A: We have replaced it.

SC9 R#2: Page 20234, Line 16: Replace "is centered in" with "focuses on"

A: The proposed word is better than our. The paper has been updated.

SC10 R#2: Page 20234, Line 20: The footnote on this page might be more appropriately added to the acknowledgments, but this is a point to take up with the editor.

A: We agree with you. However, we will wait to the Editor's decision.

Methodology

SC11 R#2: Page 20235, Line 15: It might be clearer to reword this sentences as ". . .neglect the pressure and temperature (i.e. height) dependence of the ozone absorption. . ."

A: This sentence has been reworded accordingly.

SC12 R#2: Page 20236, Line 8-9: Excluding the GFDL shortwave code from the analysis deprives the readers, especially those who may be using this parameterization in WRF, from the opportunity to understand its accuracy relative to the other methods. It is arguable that the community would be better served by including results from all of the available SW options.

A: We agree about this reviewer's suggestion and we have been working to include this parameterization in the discussion.

As a consequence, we need to update some parts of the paper:

- After reading in depth the source code, we have improved our knowledge about the ozone treatment in this radiation scheme. Therefore, we can improve the description of section 2.1.
- Following the same procedure that was described in section 2.2, we can include the analysis of the errors in the total ozone column.
- Finally, this scheme can be added in the analysis presented in section 2.3. However, this scheme does not consider the Beer-Lambert law and it computes the ozone absorption following an empirical relationship proposed by Lacis and Hansen (1974).

SC13 R#2: Page 20236, Line 10: The WRF-ARW user's guide lists the reference for the original Goddard scheme as Chou and Suarez (NASA, 1994), for the GFDL SW model as Fels and Schwarzkopf (JGR, 1981), and for RRTMG_SW as Iacono et al. (JGR, 2008).

A: We chose these references because we considered that they were representative of the approximations used in each scheme. However, we agree that it is better to use the references listed in the WRF-ARW User's Guide. They have been updated.

This review is linked with **SC3 R#1**.

SC14 R#2: Page 20236, Line 12: This reviewer's understanding of the RRTMG_SW code is that the number of sub-intervals (i.e. quadrature points) used to integrate the k-distributions in each spectral band is variable among the fourteen bands, not fixed at 16, and totals 112. This is a time saving feature of that code relative to the RRTM_SW model, which does use a fixed set of 16 quadrature points in each spectral band for a total of 224.

A: We agree about this consideration. We tried to give a simple description of the scheme but the result was a simplistic and inaccurate view. This part will be improved.

SC15 R#2: Page 20237, Line 4: Replace "81th" with "81st"

A: It has been updated.

SC16 R#2: Page 20237, Line 6: The phrase "In the first part" is vague. Please clarify.

A: We agree with you that it is not clear. It has been replaced as "In section 3.1,"

SC17 R#2: Page 20237, Line 10: Replace "composed by 37 levels" with "defined at 37 levels"

A: It has been replaced. Moreover, after during the analysis of the GFDL we found typing error. There are 81 vertical levels and 37 latitudes. The text has been checked accordingly.

SC18 R#2: Page 20237, Line 20: Replace "cover" with "covers"

A: It has been replaced.

SC19 R#2: Page 20237, Line 25: A better word than "assigned" in this sentence would be "distributed"

A: It has been updated accordingly.

SC20 R#2: Page 20238, Line 3: Add "with" before "respect"

A: It has been updated.

SC21 R#2: Page 20238, Line 12: This sentence has to be reworded. The phrase ". . .individual gas species loss progressively the hydrostatic equilibrium. . ." doesn't communicate the intended meaning.

A: This sentence has been reworded.

SC22 R#2: Page 20238, Line 16: Reword the end of this sentence to read ". . .and are monotonically decreasing"

A: It has been updated.

SC23 R#2: Page 20238, Line 19: Reword "Because of available ozone profiles. . ." as "Because the available ozone profiles. . ."

A: It has been reworded.

SC24 R#2: Page 20239, Line 6: Change "pressure at surface" to "surface pressure" **SC25 R#2:** Page 20239, Line 7: Change "pressure at surface" to "surface pressure"

A: Both have been replaced.

SC26 R#2: Page 20239, Line 8: Suggest rewording ". . .shows a dependence on the location and the season" as "varies by location and season"

A: Your suggestion sounds better than our sentence. We have reworded following your idea.

SC27 R#2: Page 20239, Line 10: Change "since" to 'from", and change "has been consistent" to "is consistent"

A: They have been updated.

SC28 R#2: Page 20239, Line 15: Suggest rewording "To discuss about the geographical. . ." to "To quantify the geographical. . ."

A: It has been updated.

SC29 R#2: Page 20239, Line 17: Suggest rewording "For the discussion about the seasonal. . ." to "In order to examine the seasonal. . ."

A: We have updated this sentence.

SC30 R#2: Page 20239, Line 20: Replace "situations" with "situation"

A: We have update this grammatical error.

SC31 R#2: Page 20239, Line 20: Suggest replacing "summarized" with "identified"

A: We agree with your suggestion.

SC32 R#2: Page 20240, Line 16: The phrase "leading a quantification about the error" is unclear and should be rewritten.

A: This part has been rewritten.

SC33 R#2: Page 20240, Line 18: Equation (5) suggests that the resulting error term on the left hand side is a function of ozone method in addition to the spatial dimensions.

A: Your are right, the nomenclature was not well defined. Equation 5 in the paper has been updated.

SC34 R#2: Page 20240, Line 23: Replace "previous" with "previously"

A: It has been updated.

SC35 R#2: Page 20240, Line 25: While it's insightful to examine the ozone method of each radiation model using a similar, simplified radiative method as described in Section 2.3, it isn't clear how this result relates to the effectiveness of each model to simulate the radiative effects of ozone within WRF. For example, are the differences in the ozone absorption related to the radiative transfer method used by each model larger, smaller or comparable to the differences caused by the ozone specification? Perhaps global calculations for a single time step with each radiation model (or at least New-Goddard and CAM) using its own ozone specification and the ozone specification of the other model would also be insightful.

A: In virtue of the Beer-Lambert law, we can analyze the ozone contribution independently of the others (see **GC1 R#2**). Moreover, real model simulations introduce other sources of error and some particularisms that were not desired for the purposes of our study.

We understand your concern when you say that it is unclear how the presented results relate to the effectiveness of each scheme to simulate the radiative effects of ozone within WRF. Nevertheless, note that, given one scheme (e.g. New Goddard), we compare two scheme outcomes (equation 22 in the old version). Variables $A_{sch,ij}(m)$ and $A_{MSR,ij}(m)$ are computed using equation 21 where $W(\lambda)$ and k_λ are provided by the scheme and TO_3 is the total ozone using the scheme ozone data and the MSR dataset, respectively.

Therefore, we intrinsically did your proposal but using the MSR as a baseline instead of permuting all the ozone datasets.

From our perspective, this is a valid procedure because the MSR dataset has been accepted by the scientific community whereas the ozone profiles in WRF do not appear in the literature and they have not been validated until our work.

In our opinion, we can include a discussion about the effectiveness of each model to simulate the radiative effects of ozone within WRF using the MSR outcomes as a baseline (i.e. $A_{MSR,ij}(m)$ from New Goddard and $A_{MSR,ij}(m)$ for CAM). This new discussion could be valuable for the readers and it is in the line of your suggestion. These considerations link with **GC2 R#1**.

We will keep in stand-by this point during the discussion of the revised version. From our point of view, this improvement implies important modifications on the structure (e.g. adding a new block).

SC36 R#2: Page 20241, Line 3: Replace "we" with "be"

A: It is a typing error. It has been updated.

SC37 R#2: Page 20241, Line 6: Reword the phrase "discussed by many literature such as"

A: The sentence has been reworded.

SC38 R#2: Page 20242, Line 3: The provided definition of W(λ) is unclear. Is this the ratio of the energy in a band dλ to the total integrated energy?

A: Yes, it is. We have tried to clarify the definition of W(λ) writing the equation explicitly in the paper.

SC39 R#2: Page 20242, Line 9: Suggest replacing "with the wavelength throughout the interval" with "on wavelength in the interval"

A: This sentence has been replaced.

SC40 R#2: Page 20244, Line 17: Reword the phrase "the minimum slant respect the normal. . ."

A: This phrase has been rewritten.

SC41 R#2: Page 20244, Line 22: Suggest rewording "using as TO3, the original and MSR datasets" as "using TO3 from the model and the MSR datasets"

A: We have updated this sentence.

SC42 R#2: Page 20245, Line 4: Clarify and reword the phrase "due to total absorptions are normalized respect. . ."

A: We agree about the inaccuracy of this sentence. In equation 11 (in the paper), we normalized the fluxes with respect to the solar radiation at the top of the atmosphere. Thus, the results from equation 21 range from 0 to 1. In equation 22, we compared two outcomes from equation 21 and, as a consequence, the bias is dimensionless. With this sentence, we tried to clarify this point to avoid any misunderstanding related to the relative error. As we detail in **SC8 R#1**, we propose to use physical units (i.e. W m^{-2}) instead of dimensionless values.

Results

SC43 R#2: Page 20245, Line 12: Move the first comma so that the sentence reads "In the RRTMG scheme, shown in Fig. 1, the lowest. . .)

A: The comma has been shifted.

SC44 R#2: Page 20246, Line 2: Replace ". . .due to the ozone profiles are limited to winter. . ." with ". . .due to the ozone profiles being limited to winter. . ."

A: It has been updated.

SC45 R#2: Page 20246, Line 4: Suggest replacing ". . .larger in the Southern during the Southern Hemisphere fall. . ." with "larger in the Southern Hemisphere from March to May. . ."

SC46 R#2: Page 20246, Line 5: Suggest replacing ". . .lower in the Northern Hemisphere during the Northern Hemisphere winter. . ." with "lower in the Northern Hemisphere from December to February. . ."

A: Your suggestions make the sentence simpler. They have been replaced.

SC47 R#2: Page 20246, Line 7: Remove "the" after "around

A: It has been replaced.

SC48 R#2: Page 20246, Line 9: Does this sentence refer to boreal spring and summer?

A: The sentence refers to the spring and summer of each Hemisphere.

In Figure 1 (G-NG-FLG), you can see negative departures in NH mid-latitude regions during April, May and June. These values drift to positive in July and August.

In contrast, you can note the reversed pattern in the SH. In October, November and December, we have negative deviations while in January and February they drift to positive values.

We have clarified the sentence to avoid any confusion.

SC49 R#2: Page 20246, Line 20: Suggest replacing "emulated" with "simulated"

A: We agree that "emulated" is not the most suitable word here, but neither "simulated" because the context is not a simulation. We propose "represented".

SC50 R#2: Page 20246, Line 27: Replace ". . .around the Greenwich's meridian. . ." with ". . .around 0deg E. . ."

A: In our opinion, we preferred using the geographical nomenclature. However, this sentence has been updated to avoid any confusion.

SC51 R#2: Page 20247, Line 5: Regarding the statement ". . .while the largest errors are observed in the RRTMG", are the authors referring to a globally weighted RMS error, or to the extreme errors? The prior text refers to larger extreme biases in the G-NG-FGL ozone method. In addition, it is recommended that this sentence be revised to refer to the biases of the ozone method used with RRTMG rather than the model itself, since the ozone specification defined in the interfacing is not strictly part of the RRTMG code itself.

A: In that paragraph we referred globally while in the G-NG-FLG we considered the extreme errors. After your review, we agree that this part must be reworded to avoid any misunderstanding.

SC52 R#2: Page 20247, Line 9: Clarify the phrase ". . .during the ending Southern Hemisphere winter and the near Southern Hemisphere spring due to the ozone hole is smoothed. . ."

A: This sentence has been clarified.

SC53 R#2: Page 20247, Line 14: Replace ". . .it is observed an underestimated region. . ." with ". . .an underestimated region is observed. . ."

A: It has been replaced.

SC54 R#2: Page 20247, Line 24: Suggest replacing "determination" with "specification"

A: We have improved this sentence.

SC55 R#2: Page 20248, Line 6: Replace "Mid-latitudes" with "Mid-latitude"

A: This error has been updated.

SC56 R#2: Page 20248, Line 10: Add "a" before "bias"

A: It has been added.

SC57 R#2: Page 20248, Line 22: Remove "the" after "around", and replace "maximum" with "maxima"

A: Both have been updated.

SC58 R#2: Page 20248, Line 27: Clarify the phrase ". . .seasonal ozone depletion occurred since winter until near spring. . ."

A: This sentence has been reworded to be more clear.

Conclusions

SC59 R#2: Page 20250, Line 5: Figures 1 and 2 suggest that this sentence should refer to the Northern Hemisphere winter.

A: Your are right, it was a typing error. We have corrected this sentence.

SC60 R#2: Page 20250, Line 9: Replace ". . .in front of the climatology" with ". . .relative to the climatology"

A: It has been replaced.

SC61 R#2: Page 20250, Line 10: The sentence that beings "Only the northern. . ." is unclear and should be reworded

A: This sentence has been rewritten.

SC62 R#2: Page 20250, Line 26: Replace "composed by" with "composed of"

A: It has been updated.

SC63 R#2: Page 20251, Line 3: Replace "address" with "addresses"

A: It has been updated.

SC64 R#2: Page 20251, Line 17: Add "the" before "underestimated"

A: It has been added.

SC65 R#2: Page 20251, Line 22: Add "As conclusion" with "In conclusion"

A: It has been replaced.

SC66 R#2: Page 20251, Line 25: The phrase "shortwave radiation at surface becoming as a relevant point due to. . ." is unclear and should be reworded

A: We agree with this reviewer opinion. We will reword this sentence to be clearer.

Tables and Figures

SC67 R#2: Figure 1: It is recommended that this be separated into two different figures and enlarged **R#2:** Figure 3: It is recommended that this be separated into two different figures and enlarged

A: We agree with these referee's ideas. However, we will wait to the Editor's decision.

Manuscript prepared for J. Name
with version 5.0 of the LaTeX class copernicus.cls.
Date: 16 December 2014

Analysis of the ozone profile specifications in the WRF-ARW model and their impact on the simulation of direct solar radiation (SC1R#1)

A. Montornès[1,2], **B. Codina**[1], **and J. W. Zack**[3]

[1]Department of Astronomy and Meteorology, University of Barcelona, Barcelona, Spain
[2]Information Services, AWS Truepower, Barcelona, Spain
[3]MESO Inc., Troy, USA

Correspondence to: A. Montornès (amontornes@am.ub.es)

Abstract.

Although ozone is an atmospheric gas with high spatial and temporal variability, mesoscale numerical weather prediction (NWP) models simplify the specification of ozone concentrations used in their shortwave schemes by using a few ozone profiles. In this paper, a two-part study is presented: (i) an assessment of the quality of the ozone profiles provided for use with the shortwave schemes in the Advanced Research version of the Weather Research and Forecasting (WRF-ARW) model and (ii) the impact of deficiencies in those profiles on the performance of model simulations of direct solar radiation. The first part compares simplified datasets used to specify the total ozone column in six ~~five~~ schemes (i.e. Goddard, New Goddard, RRTMG, CAM, GFDL and Fu–Liou–Gu) with the Multi-Sensor Reanalysis dataset during the period 1979–2008 examining the latitudinal, longitudinal and seasonal limitations in the **(SC1R#2)** ozone profile specifications ~~ozone modeling~~ of each parameterization. The results indicate that the maximum deviations are over the poles due to the Brewer–Dobson circulation and there are prominent longitudinal patterns in the departures due to quasi-stationary features forced by the land–sea distribution. In the second part, the bias in the simulated direct solar radiation due to these deviations from the simplified spatial and temporal representation of the ozone distribution is analyzed for the New Goddard and CAM schemes using the Beer–Lambert–Bouger law and for the GFDL using empirical equations. For radiative applications those simplifications introduce spatial and temporal biases with near-zero departures over the tropics throughout ~~during all~~ the year and increasing poleward with a maximum in the high middle latitudes during the winter of each hemisphere.

1 Introduction

(SC3R#2, SC4R#2)
(GC1R#1)

~~The shortwave radiation absorption by the surface and the atmosphere is the basic engine that starts the atmospheric system. In a cloudless and clear (i.e. without aerosols) sky, the most important absorbers of the solar radiation in the Earth's atmosphere are water vapor and ozone. Water vapor absorption occurs mainly in the troposphere because water sources are located on the surface. In contrast, ozone absorbs the shortwave radiation in the stratosphere becoming the major source of heating in that layer . In a dynamic frame, the ozone profile should be well detailed in numerical weather prediction (NWP) models which include vertical levels above ~ 50.~~

~~From the point of view of the radiative transfer, the optical properties of the atmosphere (i.e. optical thickness, single scattering albedo, asymmetry factor and back-scattering) are defined as a function of the atmospheric composition (i.e. gas species, aerosols, water drops or ice particles among others). Thus, the vertical characterization for the entire atmosphere arises as a critical point. For example the absorption due to the ozone in the stratosphere determines the radiative input energy in the troposphere.~~

The impact of the ozone variations in ~~on the shortwave radiation forecasts from~~ mesoscale NWP models has historically not been treated as a significant issue (Dudhia, 2014). This is because, on the one hand, these models are

not oriented to stratosphere simulations because the typical timescales in the mesoscale differ from the timescales of the interaction between the stratosphere and the troposphere. On the other hand, surface solar irradiance has a secondary role in front of other sources of error as the cloud distribution, for instance.

There is a growing interest for ~~Therefore, shortwave schemes in mesoscale NWP models simplify the ozone information reducing the computational resources of this kind of parameterization. These simplifications includes zonal averages and latitudinal, vertical and seasonal discretization that vary between shortwave parameterizations. On the other hand,~~ new applications of the mesoscale NWP models such as ~~the~~ solar energy modeling (e.g. Ruiz-Arias et al. (2013)) that requires ~~, require~~ an accurate treatment of the radiative transfer equation (RTE) throughout the entire atmosphere as well as for the study of the stratosphere (e.g. Kim and Wang (2011)) that needs an accurate computation of the solar heating rate.

Together with water vapor, ozone is the most important absorber of the solar radiation in the Earth's atmosphere in cloudless and clear (i.e. without aerosols) sky conditions.

This gas is located in two atmospheric regions with a different impact on the radiative transfer (WMO, 2011). Most ozone (∼90%) is located ~~The real ozone mixing ratio shows a high spatial and temporal variability occurring mainly~~ in the stratosphere. The region with the highest ozone concentration is commonly named as ~~defining a region denoted by~~ ozone layer and it is found between about 10 and 50 km above the surface. The remaining ozone (∼10%) is found in the troposphere. The highest values in this layer are located near the surface and they are mainly related to human activities.

The absorption of ozone in the solar spectral region occurs in three spectral bands (Inn and Tanaka, 1953; Anderson and Mauersberger, 1992): Hartley, Huggins and Chappuis. The Hartley bands are the strongest covering the ultraviolet (UV) from 200 to 300 nm. This absorption of solar flux is located primarily in the upper stratosphere and in the mesosphere. The other two bands are weaker. The Huggins bands operate in a UV region from 300 to 360 nm. Energy absorption in this spectral range occurs in the lower stratosphere and in the troposphere. Finally, the Chappius bands cover the photosynthetic active region (PAR) and the near-IR from 400 to 850 nm. The absorption by the Chappius bands is mainly located in the troposphere.

The absorption of the solar flux by ozone yields to a heating rate ranging from 10 to 30 $\mathrm{K day}^{-1}$ in the stratosphere. This absorbed energy is an important physical process in maintaining the stratospheric thermal structure (Ramanathan and Dickinson, 1979).

Stratospheric ozone ~~as reported in many studies such as in or, recently, in among others. Ozone~~ is continuously created and destroyed by photochemical processes associated with solar UV radiation. Due to the annual solar variation as well as the Earth's sphericity, significant latitudinal and seasonal variations on the ozone distribution are observed. Since the tropics receive more insolation than the poles, those ~~ultraviolet (UV) radiation. These~~ processes result in an ozone source in the tropics and a net poleward transport due to the large-scale air circulation in the stratosphere referred to ~~, which is referred to as~~ the Brewer–Dobson circulation (Brewer, 1949; Dobson, 1956). Consequently, the ozone layer in the tropics is thinner than at middle and higher latitudes where ozone is accumulated, increasing the thickness and, thus, the total ozone amount.

Seasonally, the total ozone in the tropics shows smaller variations than in the polar regions.**(SC5R#2)** The total ozone is maximum at high latitudes after ~~These results in a maximum in the total ozone during~~ the polar night because the ozone transport due to the Brewer–Dobson circulation is maximum during late fall and winter. In contrast, this circulation is weaker during summer and early fall, more in the Southern Hemisphere than in the Northern. In the polar summer, when daylight is continuous, the total ozone decreases gradually reaching the lowest value in early fall. This process is known as ozone depletion. Nevertheless, in Antarctica, an important minimum is observed in spring (September - October) as a result of chemical ozone destruction by other substances (i.e. the ozone hole).

Mesoscale NWP models do not consider prognostic or diagnostic equations for the ozone gas and its photochemical processes. In order to reduce the computational resources, the shortwave schemes in mesoscale NWP models simplify the ozone information. These simplifications include zonal averages and latitudinal, vertical and seasonal discretization that vary between shortwave parameterizations.

(GC2R#2) In fact, now there are an interest to improve the ozone representation within the WRF-ARW model. The version 3.5 (available since 2013) included a new option to share the ozone datasets between two schemes (see Sect. 2.1).

This paper presents an analysis of the strategies that are employed to specify the ozone profiles used as input into the shortwave radiation schemes in the WRF-ARW model. The analysis is split into two parts: (i) a study of the simplifications assumed in the ozone profiles and (ii) an analysis of the uncertainties **(SC6R#2)** associated with ~~added to~~ the computation of the direct solar radiation. In both, the idea is to show a global perspective (spatial and seasonal) of the limitations on modeling the ozone contribution to the radiative transfer computation in the current solar parameterizations.

In the first part, spatial and temporal deviations over the total ozone column are discussed. Each ozone profile provided with the WRF-ARW package is vertically integrated and compared with monthly averaged values from the Multi-Sensor Reanalysis (MSR) dataset (van der A et al., 2010) during the climate period 1979–2008. Surface conditions for the

vertical integration are based on the ERA-Interim[1] reanalysis (Dee et al., 2011) ~~reanalysis~~ for the same climate period.

In the second part, the effect of this error **(SC7R#2)** on ~~over~~ the direct solar radiation at the surface is computed considering an atmosphere composed only **(SC8R#2)** of ~~by~~ ozone. The analysis **(SC9R#2)** focuses on three ~~is centered in two~~ shortwave schemes: the New Goddard (Chou and Suarez, 1999; Chou et al., 2001), ~~and~~ the CAM (Collins et al., 2004) and the GFDL (Fels and Schwarzkopf, 1981). The first and second one ~~. Both~~ show the ozone mass absorption coefficient independent of the temperature and ~~the~~ pressure and consequently, the Beer–Lambert–Bouger law may be computed as a function of the total ozone column calculated in the first part. **(SC12R#2)** The third one uses empirical equations as a function of the ozone amount that allows a similar treatment.

2 Methodology

2.1 Ozone absorption in the WRF-ARW model

(SC13R#2)
(GC1R#1)

The version 3.6.1 ~~3.5~~ of the WRF-ARW model, available since 2014~~2013~~, includes seven shortwave schemes: Dudhia (available since 2000), Goddard (2000), New Goddard (2011), GFDL (2004), RRTMG (2009), CAM (2006) and FLG (2011).

The Dudhia scheme (Dudhia, 1989) is the simplest shortwave parameterization in the model without any consideration about the ozone absorption. For this reason, this parameterization is not considered in the following analyses.

(SC2R#1) The Goddard and the New Goddard schemes **(SC3R#1)** (Chou and Suarez, 1994, 1999; Chou et al., 2001) are similar because the second is an update of the first. The ozone treatment is common for both schemes and is based on Chou and Suarez (1999). From now, both schemes will be denoted as G-NG. In these schemes the solar spectrum is divided into eleven spectral bands (seven in the ultraviolet, UV, one in the visible or photosynthetic active region, PAR, and three in the near-infrared, near-IR). In the UV+PAR spectral regions, G-NG neglect the pressure and temperature (i.e. height) **(SC11R#2)** dependence of ~~effects over~~ the ozone absorption assuming a constant absorption coefficient in each spectral interval. These coefficients are obtained dividing each band into 127 narrow sub-bands with a width of $\sim 0.003\,\mu\mathrm{m}$ and using the ozone absorption coefficient given in WMO (1986). The absorption in the near-IR is added by enhancing the absorption in the PAR region, reducing the computational time. The New Goddard scheme introduces a small correction for the ozone absorption coefficient in the PAR region, from 0.0539 (cm-atm) stp^{-1} to 0.0572 (cm-atm) stp^{-1}. The effect of this correction can be neglected for the purposes of this paper considering both schemes as one. All results are based on New Goddard values since it is the newest version.

The CAM scheme (Collins et al., 2004) splits the spectrum into nineteen bands (seven for the ozone, one in the visible or PAR, seven for the water vapor, three for the carbon dioxide and one for the near-IR). The ozone absorption is computed over the seven ozone bands and over the PAR region as well. As in the previous scheme, the CAM parameterization assumes a constant ozone absorption coefficient for each band. The procedure to compute these coefficients is described in Briegleb (1992).

(SC12R#2) The GFDL scheme (Fels and Schwarzkopf, 1981) divides the spectrum in two spectral bands: one in the UV+PAR and the other in the near-IR (composed by different subdivisions). The ozone absorption occurs in ~~over~~ the UV+PAR region following the parametric formulas described in Lacis and Hansen (1974). It is noteworthy that ~~Since~~ it is the only scheme that considers the light scattering due to the ozone, explicitly. However, due to the small contribution it is not considered for the purposes of this paper. ~~oldest scheme (i.e. it was implemented in the Eta/NMM model) and the source code implementation differs from the general nomenclature in the WRF-ARW model, this parameterization is avoided in the paper.~~

The RRTMG (Iacono et al., 2008) parameterization divides the shortwave spectrum into fourteen bands covering the UV, PAR and near-IR regions. **(SC14R#2)**Each ~~and at the same time each~~ spectral band is divided in a set of sub-intervals (i.e. quadrature points) used to integrate the k-distributions for the correlated k-distribution (CKD) method detailed in Liou (1980) and Fu and Liou (1992)~~into 16 intervals used to apply the correlated-k distribution method~~. This scheme takes into account the ozone absorption coefficient dependence on pressure and temperature for each spectral band and interval. These values are stored in an external file called RRTMG_SW_DATA.

The Fu–Liou–Gu scheme (Fu and Liou, 1992; Gu et al., 2011) splits the solar spectrum into six spectral bands. As in the RRTMG parameterization, the interaction with the absorber gases is based on the CKD ~~correlated-k distribution~~ method.

Each aforementioned shortwave scheme has available different datasets reproducing ozone mixing ratio conditions in the atmosphere as a function of the pressure (i.e. vertical profile), the latitude and the season. The complexity of these datasets varies from one scheme to the other as it is summarized in Table 1 and illustrated in Fig. 1, 2 and 3. When a shortwave scheme is called by the model, the profiles are selected and interpolated into the sigma levels defined in the simulation domain.

G-NG and FLG schemes include five ozone profiles based on the same datasets **(GC1R#1)** (Fig. 1). These profiles simulate the ozone data for Tropical, Mid-latitude

[1]ECMWF ERA-Interim data used in this study have been obtained from the ECMWF data server.**(SC10R#2)**

(summer/winter) and Arctic (summer/winter) atmospheres. Thresholds to choose one profile or other are based on the latitude of the center of the domain as well as on the day of the year. Tropical regions are assumed between 30° S and 30° N without seasonal variation. In this profile, the ozone mixing ratio is maximum at 11.417 hPa with a peak of $1.29{\cdot}10^{-5}$ kgkg^{-1}. Mid-latitudes and Arctic regions are defined between 30–60 and 60–90°, respectively, considering winter and summer variations. In the Northern Hemisphere, winter is assumed between the 285th and the 80th days of the year and summer between the **(SC15R#2)** 81st ~~81th~~ and the 284th day of the year. In the Southern Hemisphere these thresholds are inverted. In both regions, the ozone layer is weaker than in tropics and it is found in a lowest altitude in summer than in winter. The highest level for all these profiles is set ~~located~~ at 0.0006244 hPa while surface conditions depend on the location and the season. In **(SC16R#2)** Sect. 3.1~~the first part~~, they are referred as G-NG-FLG.

(SC12R#2) GFDL parameterization considers ~~The GFDL parameterization includes~~ latitudinal and time variations based on the Eta/NMM model. Datasets are stored in a subroutine named ~~with resolutions of 5~~O3CLIM. This routine generates a seasonal and spatial distribution considering ~~and~~ four seasons (winter, spring, summer and fall) and 5° latitudinal distribution (Fig. 2). Ozone profiles are allocated at 81 vertical levels from 1013.25 to 0.0094 hPa. These datasets are interpolated to each grid-point of the user-defined domain. The interpolation is performed in a subroutine named as OZON2D considering the latitude and the day of the year. These datasets show a north-south symmetry between seasons with small differences that can not be appreciated in Fig. 2. Ozone in tropical regions is practically constant in all seasons while the higher latitudes experience a more variability in time. ~~, respectively.Profiles are composed by 37 vertical levels .~~

The RRTMG scheme includes two ozone profiles as a function of the season (winter or summer). Nevertheless, this granularity is useless due to the fact that the final used profile is computed as a composition of both, without considering the day of the year. Therefore, only one profile is assumed ~~considered~~ for any latitude and season (Fig. 1). **(SC5R#1)** Details about this simplification can be found in subroutine O3DATA at module_ra_rrtmg_lw.F. The highest level is located at 0.647 hPa. In the region between ~50 hPa and ~10 hPa, this profile is similar to the G-NG-FLG Tropical. Below ~50 hPa, this profile is practically the same than G-NG-FLG at Mid-latitudes while above ~10 hPa it is similar to G-NG-FLG at Mid-latitude and Arctic in winter. Since version 3.5, this scheme can utilize the ozone profiles available in the CAM scheme with the option o3input in the namelist.input file.

Finally, the CAM scheme includes several ozone profiles loaded from a binary auxiliary file called ozone_formatted with the ozone data and another two named ozone_lat.formatted and ozone_plev.formatted including latitude and pressure values, respectively. This dataset **(SC18R#2)** covers ~~cover~~ 64 latitudes with a resolution ~ 2.28° and 59 pressure levels from 1003 to 0.28 hPa for each month of the year (Fig. 3). These datasets show the highest variations in time and latitude without north-south symmetries as in GFDL's profiles. Ozone values are latitudinally interpolated for each node of the domain.

Note that with the exception of CAM, all the ozone datasets show a bad representation of the ozone depletion in Antarctica throughout winter. This simplification will lead to large errors in this region as we will discuss in Sect. 3.

2.2 Part one: study of the simplifications assumed in the ozone profiles

In this part, ozone profiles of each shortwave parameterization are vertically integrated. Next, they are **(SC19R#2)** distributed ~~assigned~~ over a regular 1° per 1° global domain for each month of a typical year **(SC6R#1)** using a bilineal interpolation. Then, these values are compared with the baseline typical year.

The reason to analyze the integrated profiles is the data availability because the real ozone profiles are limited in space and time. In general, these datasets are provided by ozone sounding stations located in a few sites around the world. Other datasets as the Binary DataBase of Profiles (Bodeker and Hassler, 2012) provide latitude and time variation profiles but neglect the longitudinal dependence and their values are the result of a regression model that fits real data. In contrast, satellite data provide a global covering but generally their algorithms compute the integrated amount.

First, let us assume one shortwave scheme. Given a vertical profile for the ozone mixing ratio called $q_{O_3}(z)$, the total ozone column TO_3, from the ground to the top of the atmosphere (TOA), is defined as

$$TO_3 = \int_0^\infty \rho q_{O_3} \mathrm{d}z, \tag{1}$$

where ρ is the dry air density and z is the height **(SC20R#2)** with respect to the ground.

Under the assumption of a well-stratified atmosphere, the pressure and the geometric height are related by the hydrostatic equation given by

$$\mathrm{d}p = -\rho g \mathrm{d}z, \tag{2}$$

where g is the gravity acceleration, assumed as a constant value.

The hydrostatic equilibrium given by Eq. (2) leads Eq. (1) to

$$TO_3 = \frac{1}{g}\int_0^{p_s} q_{O_3}(p)\mathrm{d}p. \tag{3}$$

where pressure at TOA is zero by definition and the surface pressure is denoted by p_s.

Note that the integration covers the entire atmosphere including the upper levels (i.e. above 86 km) where the **(SC21R#2)** hydrostatic equilibrium progressively gets weaken because the diffusion and ~~diffusion and the~~ vertical transport of the individual gas species become more important. In this context, the approach used in Eq. (3) is not valid ~~loss progressively the hydrostatic equilibrium~~ leading to the need of a dynamically oriented model including the diffuse separation as shown in NOAA (1976). Notwithstanding, the dry air density and the ozone mixing ratio in those layers have an order of magnitude of $10^{-6}\,\mathrm{kg\,m^{-3}}$ and $10^{-6}\,\mathrm{kg\,kg^{-1}}$, respectively, and **(SC22R#2)** are monotonically decreasing. Hence, non-hydrostatic effects may be neglected for the purposes of the current analysis.

Because **(SC23R#2)** the ~~of~~ available ozone profiles in the shortwave schemes are not analytical ~~analytic~~ functions, Eq. (3) in practice must be solved using a numerical integration scheme such as Simpson's method. Further, for an ozone profile composed by N vertical levels, Eq. (3) may be discretized such as

$$TO_3 = \frac{1}{6g}\sum_{k=1}^{N-1}(p_k - p_{k+1})(q_{O_3,k} + 0.5(q_{O_3,k} + q_{O_3,k+1}) + q_{O_3,k+1}), \tag{4}$$

where $q_{O_3,k}$ and p_k are the ozone mixing ratio and the pressure at a level k.

This vertical integration requires two boundary conditions: the ozone mixing ratio at the TOA and the **(SC24R#2)** surface pressure~~pressure at surface~~. The first one is assumed as zero (i.e. without ozone between the last available level and the TOA). The **(SC25R#2)** surface pressure ~~pressure at surface~~ requires a complex treatment since it **(SC26R#2)** varies by location and ~~shows a dependence on the location and the~~ season. This boundary is computed using the ERA-Interim reanalysis covering the climate period from ~~since~~ 1979 until 2008 (i.e. thirty years). This period is not arbitrary since it **(SC27R#2)** is ~~has been~~ consistent with the baseline data described below. Based on this period, monthly surface pressure averages are computed and used as surface conditions for the vertical integration of the ozone profiles.

From this procedure, the total ozone column for any location of the world and season can be computed. To **(SC28R#2)** quantify ~~discuss about~~ the geographical distribution of the errors, a global 1° per 1° grid is built using the latitudinal thresholds fixed in each shortwave scheme as described in Sect. 2.1. **(SC29R#2)** In order to examine ~~For the discussion about~~ the seasonal variability, values are computed throughout the twelve months of a year. Ozone profiles in some shortwave schemes like the New Goddard or the FLG are defined as a function of the day of the year instead of the month. In this **(SC30R#2)** situation~~situations~~, months are **(SC31R#2)** identified ~~summarized~~ by the 15th day of the month. This means that January is the 15th day of the year, February is the 46th day of the year, etc.

These gridded results are compared with real data. The data used as a baseline derive from the Multi-sensor reanalysis, MSR (van der A et al., 2010) during the period 1979–2008 and are monthly averaged (this dataset is provided with a monthly resolution).

The MSR was created from all available ozone column data measured by fourteen polar orbiting satellites in the near-ultraviolet Huggins band since November 1978 to December 2008, including TOMS (on the satellites Nimbus-7 and Earth Probe), SBUV (Nimbus-7, NOAA-9, NOAA-11 and NOAA-16), GOME (ERS-2), SCIAMACHY (Envisat), OMI (EOS-Aura), and GOME-2 (Metop-A). The dataset processing includes two steps. In the first one, a bias correction scheme is applied over all satellite observations based on independent ground-based total ozone data from the World Ozone and Ultraviolet Data Center. In the second step, a data assimilation process is applied using a sub-optimal implementation of the Kalman filter method and based on a chemical transport model driven by ECMWF meteorological fields. This dataset shows a bias departure less than 1 % with a root mean square standard deviation of around 2 % as compared to the corrected satellite observations used.

Therefore, for each node i (west–east direction) and j (south–north direction) and, month m, we have two datasets: one for each model under consideration, $TO_{3,\mathrm{sch},ij}(m)$, and the other one describing the baseline data, $TO_{3,\mathrm{MSR},ij}(m)$. Both datasets may be compared node by node for the entire typical year **(SC32R#2)** . We define ~~leading a quantification about the error. Hence,~~ the relative error of the parameterization $\epsilon_{ij}(m)$ as ~~may be expressed by~~

(SC33R#2)

(SC8R#1)

$$\epsilon_{sch,ij}(m) = TO_{3,\mathrm{sch},ij}(m) - TO_{3,\mathrm{MSR},ij}(m)\,\frac{TO_{3,\mathrm{sch},ij}(m) - TO_{3,\mathrm{MSR}}}{TO_{3,\mathrm{MSR},ij}(m)} \tag{5}$$

This metric will be used to discuss the simplifications assumed within the ozone column by the shortwave schemes.

2.3 Part two: an analysis of the uncertainties added to the computation of the direct solar radiation

In the second part of the study, the **(SC34R#2)** previously ~~previous~~ computed total ozone columns are used to examine the ozone absorption over the direct solar radiation and to determine the introduced bias based on climate patterns.

(GC3R#1) Given one spectral band, the downward flux $F^{\downarrow}_{\lambda}$ can be divided in two components: the direct $F^{\downarrow}_{\lambda,\mathrm{dir}}$ and the diffuse $F^{\downarrow}_{\lambda,\mathrm{dif}}$ as

$$F^{\downarrow}_{\lambda} = F^{\downarrow}_{\lambda,\mathrm{dir}} + F^{\downarrow}_{\lambda,\mathrm{dif}} \tag{6}$$

Both components require a different mathematical treatment.

Considering a direct light beam from the Sun, traveling throughout a non-scattering isotropic plane-parallel atmosphere, the monochromatic downward solar flux density, covering the spectral interval $\Delta\lambda$, may (SC36R#2) be ~~we~~ written as

$$F^{\downarrow}_{\lambda,\mathrm{dir}}(\tau_\lambda) = \mu_0 F_0(\lambda) e^{-\tau_\lambda/\mu_0}, \tag{7}$$

where τ_λ is denoted as the optical thickness for the spectral band λ and μ_0 is the cosine of the solar zenith angle. The derivation of Eq. (7) is (SC37R#2) extensively discussed in the ~~thoroughly discussed by many~~ literature such as in Chandrasekhar (1960) or in Liou (1980). This expression is commonly denoted as the Beer–Lambert–Bouguer law.

(GC3R#1) In contrast, the diffuse component requires solving the RTE in terms of a set of radiative variables as the optical thickness, the single scattering albedo and the assymetry factor. Nevertheless, the common approximation in the solar parameterizations is to assume the ozone contribution in the Rayleigh scattering term. This term is computed as a function of the air mass without any consideration about the gas species. Therefore, the diffuse flux does not depend on the ozone data and it is not analyzed in this paper.

(GC4R#1) In a non-scattering medium, when a solar beam travels throughout a layer, one part of the energy is absorbed A_λ by the medium and the other part is transmitted T_λ to the next layer (i.e. energy conservation). In other words, if we consider normalized values

$$1 = A_\lambda + T_\lambda. \tag{8}$$

As described in Liou (1980), due to the structure of the absorption lines, it is required to define the monochromatic absorptance covering the interval $\Delta\lambda$ as

$$A_{\overline{\lambda}}(\tau/\mu_0) = \int_{\Delta\lambda} (1 - e^{-\tau_\lambda/\mu_0}) \frac{\mathrm{d}\lambda}{\Delta\lambda}. \tag{9}$$

Then, assuming that the solar flux variation is small in $\Delta\lambda$, Eqs. (7) and (9) lead to

$$F^{\downarrow}_{\overline{\lambda},\mathrm{dir}}(\tau/\mu_0) \cong \mu_0 F_0(\lambda)(1 - A_{\overline{\lambda}}(\tau/\mu_0)). \tag{10}$$

Integrating Eq. (10) over the entire solar spectrum, the total flux $F^{\downarrow}_{\mathrm{dir}}(\tau/\mu_0)$ may be expressed as

$$F^{\downarrow}_{\mathrm{dir}}(\tau/\mu_0) = \int_0^\infty \mu_0 F_0(\lambda)(1 - A_{\overline{\lambda}}(\tau/\mu_0))\mathrm{d}\lambda. \tag{11}$$

Trivially, the radiation received at the TOA may be written as

$$\mu_0 F_0 = \int_0^\infty \mu_0 F_0(\lambda)\mathrm{d}\lambda. \tag{12}$$

Thus, ~~dividing~~ Eq. (11) may be expressed as ~~by Eq. (12)~~

$$F^{\downarrow}_{\mathrm{dir}}(\tau/\mu_0) \frac{F^{\downarrow}_{\mathrm{dir}}(\tau/\mu_0)}{\mu_0 F_0} = \mu_0 F_0 \int_0^\infty W(\lambda)(1 - A_{\overline{\lambda}}(\tau/\mu_0))\mathrm{d}\lambda, \tag{13}$$

where $W(\lambda)$ is the ratio of the extraterrestrial energy in a band $\mathrm{d}\lambda$ as (SC38R#2)

$$W(\lambda) = \frac{F_0(\lambda)}{F_0}. \tag{14}$$

Defining the total absorption $A(\tau/\mu_0)$ as

$$A(\tau/\mu_0) = \mu_0 F_0 \int_0^\infty W(\lambda) A_{\overline{\lambda}}(\tau/\mu_0)\mathrm{d}\lambda, \tag{15}$$

Eq. (13) may be written as

$$F^{\downarrow}_{\mathrm{dir}}(\tau/\mu_0) \frac{F^{\downarrow}_{\mathrm{dir}}(\tau/\mu_0)}{\mu_0 F_0} = \mu_0 F_0 1 - A(\tau/\mu_0). \tag{16}$$

Let us now consider the particular case in which the dependence of the optical thickness (SC39R#2) on wavelength in ~~with the wavelength throughout~~ the interval $\Delta\lambda$ can be neglected. In that case, Eq. (9) may be written as

$$A_{\overline{\lambda}}(\tau/\mu_0) = 1 - e^{-\tau_\lambda/\mu_0}. \tag{17}$$

Leading Eq. (11) to

$$F^{\downarrow}_{\mathrm{dir}}(\tau/\mu_0) \frac{F^{\downarrow}_{\mathrm{dir}}(\tau/\mu_0)}{\mu_0 F_0} = \mu_0 F_0 \int_0^\infty W(\lambda) e^{-\tau_\lambda/\mu_0}\mathrm{d}\lambda. \tag{18}$$

Therefore, from Eqs. (16) and (18), the total absorption can be isolated and computed as

$$A(\tau/\mu_0) = \mu_0 F_0 1 - \mu_0 F_0 \int_0^\infty W(\lambda) e^{-\tau_\lambda/\mu_0}\mathrm{d}\lambda \tag{19}$$

(SC7R#1) The optical thickness is a function of the gases and particles that compose the atmosphere and of the absorption coefficient cross section of each one. A wide

used approximation is to assume that a set of absorbers are independent of one another. Therefore, the radiative schemes compute the the total optical thickness τ_λ as the sum of different contributions such as ozone $\tau_{\lambda,O3}$, water vapor $\tau_{\lambda,wv}$, clouds $\tau_{\lambda,cld}$, aerosols $\tau_{\lambda,aer}$ and others:

$$\tau_\lambda = \tau_{\lambda,O3} + \tau_{\lambda,wv} + \tau_{\lambda,cld} + \tau_{\lambda,aer} + ... \quad (20)$$

Thus, considering equation 20, the contribution of each absorber to the absorption can be analyzed independently in Eq. 19.

In the particular case of the ozone, the optical thickness defined from the TOA to a level z may be expressed as

$$\tau_{\lambda,O3}(z) = \int_z^\infty k_\lambda \rho q_{\mathrm{O_3}} \mathrm{d}z, \quad (21)$$

where k_λ denotes the mass absorption cross section and ρ is the dry air density. Note that this integral requires the vertical information of the ozone mixing ratio and the dry air density.

Moreover, k_λ is dependent on temperature and pressure as can be demonstrated in virtue of the kinetic theory of gases. Hence, as $\tau_{\lambda,O3}$ is a function of the height z and this is a function of the temperature and pressure, the integral can not be computed without a detailed information about k_λ.

Regarding the spectral computation given by equation 19, the most accurate method is the line-by-line (LBL) calculation. However, this method is not computationally feasible because it would require many thousands of computations at each grid-point. Instead of this, some approximations are assumed in terms of the gas and its spectral behavior.

Ozone absorption coefficient cross section shows a smooth variation with the wavelength (Inn and Tanaka, 1953). Hence, an effective k_λ is defined for each spectral band. This coefficient is previously computed using the LBL at a reference pressure and temperature and then, scaled to the pressure and temperature of each values in order to consider the dependency on these magnitudes.

Goddard, New Goddard and CAM follow this approach without scaling k_λ as detailed in Chou and Suarez (1999) and Briegleb (1992).

Thus, the absorption coefficient becomes temperature and pressure independent ~~If a medium is homogeneous, the absorption coefficient becomes independent of the temperature and the pressure~~ and Eq. (21) may be expressed by

$$\tau_{\lambda,O3}(z) = k_\lambda \int_z^\infty \rho q_{\mathrm{O_3}} \mathrm{d}z. \quad (22)$$

~~The atmosphere is not homogeneous and not all the shortwave schemes in the WRF-ARW model use this approach. As aforesaid in Sect. 2.1, only the New Goddard and the CAM parameterizations consider k_λ as a constant with height.~~

Extending the integral over the entire atmosphere and assuming the hydrostatic equilibrium given by Eq. (2), Eq. (22) may be written as

$$\tau_{\lambda,O3}(p_\mathrm{s}) = \frac{k_\lambda}{g} \int_0^{p_\mathrm{s}} q_{\mathrm{O_3}} \mathrm{d}p. \quad (23)$$

In virtue of Eq. (3), the optical thickness may be expressed as

$$\tau_{\lambda,O3}(p_\mathrm{s}) = \frac{k_\lambda}{g} TO_3(p_\mathrm{s}). \quad (24)$$

Substituting Eq. (24) into Eq. (19), the total absorption may be written as

$$A(\tau_{\lambda,O3}/\mu_0) = \mu_0 F_0 (1 - \int_0^\infty W(\lambda) e^{-\frac{k_\lambda}{g\mu_0} TO_3} \mathrm{d}\lambda). \quad (25)$$

The necessary information to compute the $A(\tau/\mu_0)$ in Eq. (25) are the TO_3, $W(\lambda)$, k_λ and μ_0. Information about the TO_3 can be obtained from Sect. 2.2. The $W(\lambda)$, k_λ are data available in the source code of each shortwave scheme (i.e. New Goddard and CAM). Finally, the cosine of the solar zenith angle μ_0 may be computed as a function of the latitude, the longitude, the hour and the day of the year.

From the expression 25, we can conclude that, given a fixed wavelength, there are two variables that may change the ozone absorption over the globe. On the one hand, the cosine of the solar angle increases the absorption as solar beams travel throughout a longer path when the Sun is near to the horizon than when is normal to the surface. On the other hand, the total ozone column increases or decreases the opacity of the atmosphere, absorbing more or less energy.

Regarding RRTMG and FLG, both consider the absorption coefficient dependence on pressure and temperature as we explained in Sect. 2. Therefore, the approximation assumed in Eq. (22) is not valid. For this reason these schemes are not considered in the *Part two*.

(SC12R#2) The aforementioned procedure can not be applied to GFDL because this scheme does not calculate the Beer's Law explicitly. Instead of that, this scheme uses empirical relationships proposed by Lacis and Hansen (1974). Following these expressions, the ozone absorption is computed as

$$A^{uv}_{o3}(x) = \frac{1.082x}{(1+138.6x)^{0.805}} + \frac{0.0658x}{1+(103.6x)^3} \quad (26)$$

in the UV spectral region, and

$$A_{o3}^{vis}(x) = \frac{0.02118x}{1+0.042x+0.000323x^2} \quad (27)$$

in the PAR region.

In equations 26 and 27, x is defined as the ozone amount u_{O3} traversed by the solar beam in a defined layer as

$$x = u_{O3}M, \quad (28)$$

where M is the magnification factor proposed by Rodgers (1979) as

$$M = \frac{135}{(1224\mu_0^2+1)^{1/2}}. \quad (29)$$

Therefore, considering the UV and PAR bands as a single one, the total absorption is

$$A(x) = A_{o3}^{uv}(x) + A_{o3}^{par}(x). \quad (30)$$

Note that if we consider the entire atmosphere, u_{O3} it is directly $TO3$ as in the aforesaid schemes. Thus, although this parameterization does not compute the Beer's Law, an analogous procedure can be applied. ~~To avoid day/night problems throughout the zonal direction, all longitudes assume midday in local time (i. e. the minimum slant respect the normal in the optical thickness) . In the meridional direction, those latitudes showing a solar zenith angle greater than 80are considered as night (i. e. polar night).~~

Under these considerations, given a shortwave scheme, Eq. (25)[2] is applied over each node of the grid for all months. To calculate the bias, the absorption is computed using **(SC41R#2)** ~~as~~ TO_3 from the model ~~, the original~~ and MSR datasets. For a given month m, let us assume $A_{\mathrm{sch}}(i,j)(m)$ and $A_{\mathrm{MSR}}(i,j)(m)$ the absorption result for the ozone dataset of the scheme and the MSR, respectively, for a node at i (west–east direction) and j (south–north direction). The bias of the parameterization $\mathrm{BIAS}_{ij}(m)$ may be defined as
(SC42R#2)
(SC8R#1)

$$\mathrm{BIAS}_{ij}(m) = A_{\mathrm{sch},ij}(m) - A_{\mathrm{MSR},ij}(m) \quad (31)$$

(SC40R#2) To avoid day/night problems throughout the zonal direction, all longitudes assume midday in local time (i.e. the minimum slant path). In the meridional direction, those latitudes showing a solar zenith angle greater than 80° are considered as night (i.e. polar night).

[2] Eq. (30) in GFDL.

Considering Eq. (8), an overestimation (underestimation) in the ozone absorption implies that the modeled atmosphere is too much opaque (transparent) and consequently, the ozone contribution to the direct flux is underestimated (overestimated) in the same magnitude~~Note that this metric is not normalized but it has units of parts per unit due to total absorptions are normalized respect to the flux at the TOA~~.

3 Results

(SC8R#1)

3.1 Part one: study of the simplifications assumed in the ozone profiles

In this section, ozone profiles provided with the WRF-ARW model are evaluated following the procedures described in Sect. 2.2. We first focus on detailing results for each dataset (i.e. RRTMG, G-NG-FLG, CAM and GFDL~~and CAM~~) over the globe. After this, there is a general discussion of the spatial and temporal deviation patterns.

In the RRTMG scheme **(SC43R#2)** , shown ~~shown,~~ in Fig. 4~~??~~, the lowest deviations of the total ozone column are observed along the mid-latitudes of each hemisphere during the respective (i.e. Northern or Southern Hemisphere) winter and spring, lower in the Northern than in the Southern. The global minimum is reached in May, in Siberia (-30 DU~~8~~) and along Europe (between -20 and $+20$ DU~~3~~). With the exception of the ozone hole, the largest departures in the total ozone column are observed along the tropics ($+100$ ~~35~~ to $+150$ DU~~60~~) as a function of the month. An asymmetry with respect to the Equator line is observed, reaching the highest overestimation in the winter hemisphere due to the low ozone production. The global maximum is observed over Antarctica in September ($+170$ ~~90~~ to $+190$ DU~~100~~) and October ($+180$ ~~90~~ to $+200$ DU~~130~~).

The G-NG-FGL results, Fig. 5~~??~~, show a strong difference between tropics and mid-latitudes ~~the tropics and the midlatitudes~~ and high latitudes. The tropics show the best accuracy over the year with values between -20 ~~10~~ and $+20$ DU ~~2~~with a tendency to underestimate the total ozone column values. Seasonally, positive and negative departures are observed over the summer and winter hemispheres, respectively. Mid-latitudes and high latitudes show a high seasonal variability due to the ozone profiles **(SC44R#2)** being ~~are~~ limited to winter or summer (Table 1). The mid-latitude winter profile shows positive deviations over both hemispheres, larger in the Southern **(SC45R#2)** Hemisphere from March to May ~~during the Southern Hemisphere fall~~ ($+40$ ~~35~~ to $+120$ DU~~50~~) and lower in the Northern Hemisphere **(SC46R#2)** from December to February ~~during the Northern Hemisphere winter~~ (-60 ~~15~~ to -0 DU ~~5~~over the eastern side of Asia, -20 ~~10~~ to 0 DU over the northern side of the United States and 0 to $+100$ DU ~~30~~over the rest). In January a near-

zero belt around (SC47R#2) ~~the~~ 60° N is observed, which expands southward during February and March. In contrast, the mid-latitude summer profile drifts from slightly negative departures during the spring to slightly positive deviations in summer (SC48R#2) of each Hemisphere. The Arctic winter profile shows positive deviations in ~~over~~ both hemispheres. The greatest values in the Northern Hemisphere are observed in October (around +200 DU in ~~70 to +80over~~ Greenland and the Scandinavian Peninsula) while the largest deviations in the Southern Hemisphere are reached in September (+260 ~~135~~ to +300 DU ~~155~~over Antarctica). The Arctic summer profile shows different patterns in each hemisphere. In the Northern Hemisphere, negative deviations (−80 ~~15~~ to −20 DU~~5~~) are observed during the spring drifting into positive departures in summer (+20 ~~5~~ to +40 DU ~~15~~in July, +40 ~~10~~ to +80 DU ~~20~~in August and +60 ~~15~~ to +80 DU ~~25~~in September) with near-zero values in June. The Southern Hemisphere shows positive departures during all the months reaching the minimum value in December in ~~maximum value in October over~~ Antarctica (+20 ~~95~~ to +60 DU~~105~~).

In ~~Finally, in~~ the CAM case, Fig. 6~~??~~, the latitudinal and seasonal variations are well (SC49R#2) represented with typical ~~emulated with~~ departures between the −40 ~~10~~ and the +40 DU ~~10~~with a clear overestimation. The largest departures are a result of the lack of consideration of the longitudinal ozone variations in the datasets available to the shortwave radiation schemes. Departures between +60 ~~20~~ and +80 DU ~~25~~are reached over January and February in a defined region between Greenland and the Scandinavian Peninsula. Moreover, the east-west variations due to the ozone hole produce a high overestimated region (between +60 ~~30~~ and +80 DU ~~40~~with peaks above (SC50R#2) +90 DU) around 0° E ~~45) around the Greenwich's meridian~~ and a high underestimation region (−60 ~~20~~ to −20 DU~~10~~) in the opposite side of Antarctica (i.e. 180 ° E). In November and December, an overestimated region (+0 ~~15~~ to +20 DU) is observed over the Mediterranean basin and over the Sahara.

(SC12R#2) Finally, in GFDL scheme (Fig. 7), the total ozone column is slightly underestimated in the tropics and strongly overestimated poleward. The lowest negative biases are observed from December to February (-20 to 0 DU) with a maximum at the Equator in a region between Africa and South America (-60 to -20 DU). During the Northern Hemisphere spring and summer, the negative values increase in magnitude as well as in area reaching higher latitudes (-50º S to 50º N) with peaks reaching -80 DU at the end of summer. From October to December, this underestimated area is progressively weakened. In mid-latitudes, the pattern differs from the Northern Hemisphere to the Southern one. In the first one, a dipole between the Atlantic and the Eastern Asia is observed from December to March. A positive area is observed in the Atlantic region with values from +60 to +100 DU. In contrast, the Eastern Asia shows negative values from -80 to -40 DU. This pattern is weaker during the Northern Hemisphere spring and fall, disappearing in summer. In the Southern Hemisphere, positive errors are observed without a longitudinal dependency. The lowest biases are produced from January to March (+20 to +100 DU) drifting to higher values from April to December (+80 to +120 DU) during the Southern Hemisphere spring and are maximum in summer and fall reaching peaks greater than +140 DU. The polar regions show a strong seasonal pattern with a positive bias. In both hemispheres, the lowest values are reached in the respective summer while the highest values are produced during the polar night. In the Arctic, the bias is lower than in the Antarctica. From December to February, the Arctic regions reach errors between +100 and +180 DU. In contrast, from July to September, the error ranges from +20 to +60 DU. The Antarctica shows the highest bias from September to October ranging from +280 to +300 DU being the parameterization with the highest errors. The lowest values are experienced during the Southern Hemisphere summer being larger than in the Arctic.

(SC51R#2) Latitudinally and seasonally, the distribution of the departures shows a logical coherence with the quality of the ozone profiles available in each shortwave scheme. Thus, the ozone dataset in the CAM scheme shows the lowest deviations while the largest global errors are observed in the RRTMG. Generally, the total ozone column is overestimated by all the analyzed schemes with the exception of some locations, especially, for the G-NG-FGL profiles. The largest extreme departures are observed over (SC52R#2) Antarctica between the ending ~~during the ending Southern Hemisphere~~ winter and the near spring of the Southern Hemisphere given that ~~Southern Hemisphere spring due to~~ the ozone hole is weaken ~~smoothed~~ in all the ozone datasets.

Longitudinally, similar distribution patterns can be observed for all the shortwave schemes because all of them assume meridional averages in the ozone mixing ratio. Two zones may be discussed. Firstly, during the Northern Hemisphere fall and winter, (SC53R#2) ~~it is observed~~ an underestimated region is observed between the north-eastern side of Asia and the north-western side of Canada as well as an overestimated region between Greenland and the Scandinavian Peninsula. This pattern reflects the quasi-stationary features of the upper-air circulation due to the sea–land distribution in the Northern Hemisphere as discussed in Dütsch (1974) or in Fusco and Salby (1999). Secondly, strong longitudinal gradients in the distribution of the errors are observed over Antarctica due to the ozone hole in September and October. In the other locations, the east-west distribution of the errors may be neglected.

3.2 Part two: an analysis of the uncertainties added to the computation of the direct solar radiation

As previously noted in Sect. 2.3, the errors in the (SC54R#2) specification ~~determination~~ of the ozone profiles are propagated in the shortwave radiation results. In this section, sys-

tematic biases introduced in the modeling of the direct solar radiation are discussed focusing on three ~~two~~ schemes: New Goddard, CAM and GFDL~~and CAM~~. First, a detailed description of the uncertainties over the globe is shown. Then, a general view of those limitations and their implications is discussed.

In the New Goddard scheme (Fig. 8), the bias in the total absorption ~~with respect to the radiation at TOA~~ ranges from -3 ~~1.0~~ to $+3\,\mathrm{Wm^{-2}}$ ~~1.0~~reaching peaks near $+6\,\mathrm{Wm^{-2}}$ ~~2.0~~values close to the poles. The absorption is slightly underestimated in the tropics for the entire year. **(SC55R#2)** Mid-latitude ~~Mid-latitudes~~ regions show overestimated values in winter, more homogeneous and higher in the Southern Hemisphere than in the Northern, ranging from $+0$ to $+2\,\mathrm{Wm^{-2}}$~~0.7~~. Near-zero values are observed over North America and Asia and extended over Europe in March. An exception of this winter pattern occurs over the eastern side of Asia where **(SC56R#2)** a bias greater than $-1\,\mathrm{Wm^{-2}}$ ~~0.4~~is observed. During the spring, negative and near-zero departures in the bias are observed over both hemispheres, higher in the Northern (from $-2\,\mathrm{Wm^{-2}}$ ~~0.4~~in April to near-zero values in June) than in the Southern (from slightly negative in October to near-zero in December). In summer, the departures drift from near-zero biases during the early season to positive values at the end of the summer. As in the winter season, the bias is higher in the Southern Hemisphere. During the fall, the largest negative bias is observed over both hemispheres reaching the maximum during the first months.

The CAM scheme (Fig. 9) shows the lowest biases in the total absorption of the solar beam due to the ozone. The bias is clearly positive during the whole year with the exception of the northern side of the Pacific Ocean from October to March reaching deviations of $-1\,\mathrm{Wm^{-2}}$ ~~1.0~~in December over the Asian coast and, in some regions over Antarctica from August to October, reaching departures around ~~the~~ $-1\,\mathrm{Wm^{-2}}$~~0.5~~. Two positive **(SC57R#2)** maxima ~~maximum~~ are observed, one over Arctic from January to March with peaks around $+2\,\mathrm{Wm^{-2}}$ ~~1.0~~and, the other over Antarctica from September to November reaching a bias of $+0.5\,\mathrm{Wm^{-2}}$. Although this scheme has the highest latitudinal resolution, the largest deviations are observed throughout high-latitudes because the ozone profiles simplify the meridional variations produced by the seasonal ozone depletion **(SC58R#2)** that appears from ~~occurred since~~ winter until near spring (Southern and Northern Hemisphere).

(SC12R#2) In GFDL (Fig. 10), absorption biases show a different pattern between the tropics and the other latitudes. In the tropics, the bias is slightly negative throughout all the year. The values range from -3 $\mathrm{Wm^{-2}}$ and 0 $\mathrm{Wm^{-2}}$. In contrast, the absorption is strongly overestimated in mid-latitudes and polar regions with typical departures between 0 $\mathrm{Wm^{-2}}$ and +5 $\mathrm{Wm^{-2}}$. The highest departures are observed over Antarctica from September to November with values between +6 $\mathrm{Wm^{-2}}$ and +12 $\mathrm{Wm^{-2}}$ and in Arctic from February to April with departures between +3 $\mathrm{Wm^{-2}}$ and +6 $\mathrm{Wm^{-2}}$ being maxima in the Scandinavian Peninsula. Mid-latitude regions show a similar distribution than CAM. Whereas the Southern Hemisphere shows a low dependence on longitude, the Northern one shows a pattern with a dependence on space (i.e. meridional) and time. From October to April, two different regions, positive and negative, are observed between Atlantic and Pacific, respectively. During the other months, the meridional differences are lower and the bias tends to be slightly negative in all latitudes.

The results from this part of the study are generally consistent with the ozone column deviation results shown in Fig. 5, 6 and 7~~Figs. ?? (G-NG-FLG) and ??~~. Both schemes tend to overestimate the absorption with lower departures in the tropics than in the middle or high latitudes and a maximum over Antarctica during the early Southern Hemisphere spring. As opposed to the results in Sect. 3.1, the impact of these errors on the simulation of the shortwave irradiance at the surface is linked to the Sun's position. The highest ozone biases in the poles are masked by their coincidence with the polar night. However, the low solar elevation angles at high latitudes results in a higher sensitivity to the ozone datasets in these latitudes. These factors combine to produce the largest meridional gradients in the errors in the modeling of direct solar radiation in the high latitudes during the winter season of each hemisphere.

4 Conclusions

Two sets of conclusions can be derived from the results of the analysis presented in this paper. The first set is related to the quality of the ozone concentration datasets available to the WRF-ARW mesoscale model and the second set is associated with the impact of these deficiencies in representing the spatial and temporal variations of the ozone profiles on the performance of the shortwave radiation schemes available to WRF-ARW model users.

The key point is that the analysis indicates that the ozone profiles available to ~~in~~ the WRF-ARW package are a poor representation of the ozone distribution over the planet during a typical year. These datasets assume zonal averages in the ozone mixing ratio and describe the anomalies in latitude and in time with a low resolution.

In general, the largest deviations are observed over the polar latitudes during the winter of each hemisphere due to the ozone depletion, greater in Antarctica than in Arctic.

All the WRF-ARW ozone datasets that were analyzed in this study exhibited similar longitudinal error patterns. The error patterns were more prominent in the Northern Hemisphere due to the quasi-stationary features associated with the land–sea distribution that are not captured in the ozone profiles. As consequence, a systematic underestimation of the total ozone column is observed in a region between the east of Asia (i.e. eastern Russia) and the west of North Amer-

ica (i.e. Alaska and Western Canada) during the (SC59R#2) Northern ~~Southern~~ Hemisphere winter and near spring. In contrast, a systematic overestimation occurs in a region defined between Greenland and the Scandinavian Peninsula during the Southern Hemisphere fall and near winter.

The RRTMG, with a single ozone profile for all the latitudes and seasons, is the shortwave scheme with the poorest ozone resolution and the largest departures (SC60R#2) relative to ~~in front of~~ the climatology. Only the (SC61R#2) ~~northern~~ mid-latitudes in the Northern Hemisphere show small deviations for being calibrated in these ~~as consequence that was calibrated in that~~ latitudes.

The ozone profiles used by the Goddard, New Goddard and the Fu–Liou–Gu consider five ozone profiles: tropical, mid-latitude (winter/summer) and Arctic (winter/summer) for both hemispheres. This discretization shows ~~show~~ better results in the Northern Hemisphere than in the Southern Hemisphere. The tropical profile shows a systematic underestimation of the ozone amount over any longitude, greater in the summer hemisphere, near-zero in the winter hemisphere and practically homogeneous during the equinoxes. This underestimation pattern is directly linked to the obliquity of the ecliptic and the available insolation producing ~~which produce~~ more ozone in summer than in winter. Positive departures are observed over the mid-latitudes in winter and ~~in~~ summer, better for the second one in ~~in the second for~~ both hemispheres. Negative deviations are observed during spring while the worst results of the year are obtained during fall. A similar pattern is observed in the polar regions with greater differences between the northern and the southern as discussed at the beginning of this section.

Finally, the CAM shortwave parameterization shows the lowest departures in the total ozone column. This scheme, composed (SC62R#2) of ~~by~~ 64 ozone profiles with a monthly temporal resolution, captures a great part of the ozone variations over the globe. The largest deviations are observed throughout the longitudes because of the zonal averages in the profile datasets. The highest zonal gradients in the errors are observed over the poles during the winter season of each hemisphere.

The second set of conclusions (SC63R#2) addresses ~~address~~ the impact of the deficiencies in the specification of the ozone distribution on the simulation of the shortwave radiation. A key point is that the impact of errors in the representation of the spatial and temporal distribution of ozone on the model's simulation of shortwave radiation is determined by multiple factors and it is not a simple function of the errors in the ozone profiles. For example, the largest errors in the ozone profiles were determined to be in the Polar Regions during winter. However, the impact of these errors on the simulation of shortwave radiation are masked by the coincidence of these errors with the polar night. On the other hand, the low solar elevation angles at high latitudes result in a higher sensitivity of the shortwave radiation schemes to the ozone profiles in these latitudes. These factors combine to produce the largest meridional gradients in the errors in the simulations of shortwave radiation in the high latitudes during the winter season of each hemisphere.

The lowest biases in the absorption of the solar direct beam occur over the tropics (Fig. 8, 9 and 10??) with near-zero departures. In contrast, the largest biases are observed poleward during the winter of each hemisphere. Longitudinally, (SC64R#2) the underestimated ozone region over the northern Pacific produces important biases in the absorption.

The CAM parameterization shows lower biases (-1 to $1\,\mathrm{Wm^{-2}}$) than ~~) than the~~ New Goddard scheme (-3 ~~1~~ to $3\,\mathrm{Wm^{-2}}$) and GFDL (-2 to $2\,\mathrm{Wm^{-2}}$) with the same spatial and temporal distribution found in the total ozone errors as expected. The greatest overestimation is located over Antarctica from September to November being GFDL the worst parameterization (8 to $12\,\mathrm{Wm^{-2}}$) followed by New Goddard (1 to $5\,\mathrm{Wm^{-2}}$) and CAM (0 to $1\,\mathrm{Wm^{-2}}$).

(SC65R#2) In ~~As~~ conclusion, the ozone profiles provided with the WRF-ARW package have significant limitations because of their simplified representation of spatial and temporal variability of ozone concentrations. (SC66R#2) These limitations introduce systematic biases in the modeling of shortwave radiation at surface that can be easily reduced with more sophisticated datasets.~~Those limitations introduce systematic biases in the modeling of shortwave radiation at surface becoming as a relevant point due to the growing interest in solar energy applications.~~(GC5R#1), (GC2R#2) As we explained in Sect. 2.1, the RRTMG scheme can utilize the ozone profiles available in CAM since version 3.5. The set of results in this paper confirm that this improvement is on the right path and it should be extended to the other solar parameterizations.

In virtue of the conclusions presented in this paper, a future study of the daily variation in the deviations could be valuable for solar short-term forecasting, since introduced biases could be corrected by using different statistical post-processing approaches (e.g. Model Output Statistics, MOS). Furthermore, the ozone profiles could be validated using real ozone soundings in order to determine the contribution to the solar heating rate error, important for stratospheric modeling, as it was presented in the Introduction.

Acknowledgements. The research leading to these results has received funding from the Departament d'Economia i Coneixement de la Generalitat de Catalunya in the frame of the Talent empresa programme (grant: 2010-TEM-49).

References

references

Anderson, S. M. and Mauersberger, K.: Laser measurements of ozone absorption cross sections in the Chappuis band. J. Geophys. Res. Lett., 19, 933-936,

doi:http://dx.doi.org/10.1029/92GL0078010.1029/92GL00780, 1992.

Bodeker, G. and Hassler, B.: Bodeker Scientific Global Vertically Resolved Ozone Database, [Internet], NCAS British Atmospheric Data Centre, 2012, 2014-12-04. Available from http://catalogue.ceda.ac.uk/uuid/9a2438602c2b534f54d81e54b9d98d75

Brewer, A.: Evidence for a world circulation provided by the measurements of helium and water vapour distribution in the stratosphere, Q. J. Roy. Meteor. Soc., 75, 351–363, 1949.

Briegleb, B. P.: Delta–Eddington approximation for solar radiation in the NCAR Community Climate Model, J. Geophys. Res., 97, 7603–7612, 1992.

Chandrasekhar, S.: Radiative Transfer, Dover Publications, New York, 1960.

ChouChipperfield, M.-D. and Suarez, M. J.: An efficient thermal infrared radiation parameterization for use in general circulation models, NASA Tech. Memo, NASA/GSFC, 104606, 3, 1994.
and Jones, R.: Relative influences of atmospheric chemistry and transport on Arctic ozone trends, Nature, 400, 551–554, , 1999.

Chou, M.-D. and Suarez, M. J.: A Solar Radiation Parameterization for Atmospheric Studies, NASA Tech. Memo, NASA/GSFC, 104606, 40, 1999.

Chou, M.-D., Suarez, M. J., Liang, X.-Z., and Yan, M. M.-H.: A thermal infrared radiation parameterization for atmospheric studies, NASA Tech. Memo, 104606, 56, available at: http://ntrs.nasa.gov/search.jsp?R=20010072848 (last access: 1 August 2014), 2001.

Collins, W. D., Rasch, P. J., Boville, B. A., Hack, J. J., McCaa, J. R., Williamson, D. L., Kiehl, J. T., Briegleb, B., Bitz, C., Lin, S., Zhang, M., and Dai, Y.: Description of the NCAR Community Atmosphere Model (CAM 3.0), NCAR Tech. Note NCAR/TN-464+ STR, Boulder, Colorado, 2004.

Dee, D. P., Uppala, S. M., Simmons, A. J., Berrisford, P., Poli, P., Kobayashi, S., Andrae, U., Balmaseda, M. A., Balsamo, G.,Bauer, P., Bechtold, P., Beljaars, A. C. M., Berg, L., Bidlot, J., Bormann, N., Delsol, C., Dragani, R., Fuentes, M., Geer, A. J., Haimberger, L., Healy, S. B., Hersbach, H., Hólm, E. V., Isaksen, L., Kållberg, P., Köhler, M., Matricardi, M.,McNally, A. P., Monge-Sanz, B. M., Morcrette, J.-J., Park, B.-K., Peubey, C., Rosnay, P., Tavolato, C., Thépaut, J.-N., and Vitart, F.: The ERA-Interim reanalysis: configuration and performance of the data assimilation system, Q. J. Roy. Meteor. Soc., 137, 553–597, doi:http://dx.doi.org/10.1002/qj.82810.1002/qj.828, 2011.

Dobson, G. M.: Origin and distribution of the polyatomic molecules in the atmosphere, Proc. R. Soc. Lon. Ser.-A, 236, 187–193, 1956.

Dudhia, J.: Numerical study of convection observed during the winter monsoon experiment using a mesoscale two-dimensional model, J. Atmos. Sci., 46, 3077–3107, doi:http://dx.doi.org/10.1175/1520-0469(1989)046%3C3077:NSOCOD%3E2.0.CO;210.1175/1520-0469(1989)046<3077:NSOCOD>2.0.CO;2, 1989.

Dudhia, J.: A history of mesoscale model development, Asia-Pac. J. Atmos. Sci., 50, 121–131, doi:http://dx.doi.org/10.1007/s13143-014-0031-810.1007/s13143-014-0031-8, 2014.

Dütsch, H.: The ozone distribution in the atmosphere, Can. J. Chem., 52, 1491–1504, 1974.

Fels, S. and Schwarzkopf, M.: An efficient, accurate algorithm for calculating CO2 15 μm band cooling rates, J. Geophys. Res., 86, C2, 1205–1232, 1981.

Fu, Q. and Liou, K., N.: On the correlated k-distribution method for radiative transfer in nonhomogeneous atmospheres, 49, 22, 2139-2156, doi:http://dx.doi.org/10.1175/1520-0469(1992)049%3C2139:OTCDMF%3E2.0.CO;210.1175/1520-0469(1992)049<2139:OTCDMF>2.0.CO;2, 1992.

Fusco, A. and Salby, M.: Interannual variations of total ozone and their relationship to variations of planetary wave activity, J. Climate, 12, 1619–1629, 1999.

Gu, Y., Liou, K., Ou, S., and Fovell, R.: Cirrus cloud simulations using WRF with improved radiation parameterization and increased vertical resolution, J. Geophys. Res., 116, D06119, doi:http://dx.doi.org/10.1029/2010JD01457410.1029/2010JD014574, 2011.

Iacono, M. J., Delamere, J. S., Mlawer, E. J., Shephard, M. W, Clough, S. A. and Collins, W. D.: Radiative forcing by longlived greenhouse gases: Calculations with the AER radiative transfer models, J. Geophys. Res., 113, D13103, doi:http://dx.doi.org/10.1029/2008JD00994410.1029/2008JD009944, 2008.

Inn, E. C. and Tanaka, Y.: Absorption coefficient of ozone in the ultraviolet and visible regions, J. Opt. Soc. Am., 43, 10, 870–872, 1953.

Kim, H. J. and Wang, B.: Sensitivity of the WRF model simulation of the East Asian summer monsoon in 1993 to shortwave radiation schemes and ozone absorption, Asia-Pac. J. Atmos. Sci., 47, 2, 167–180, 2011.

Lacis, A. A. and Hansen, J.: A parameterization for the absorption of solar radiation in the Earth's atmosphere, J. Atmos. Sci., 31, 118–133, 1974.

Liou, K. N.: An Introduction to Atmospheric Radiation, vol. 84, International Geophysics Series, Academic Press, New York, 1980.
Mlawer, E. J., Taubman, S. J., Brown, P. D., Iacono, M. J., and Clough, S. A.: Radiative transfer for inhomogeneous atmospheres: RRTM, a validated correlated-k model for the longwave, J. Geophys. Res., 102, 16663–16682, 1997.

NOAA: US Standard Atmosphere, 1976, Tech. rep., NOAA-S/T, U.S. Government Printing Office, Washington, D.C., 1976.
Parrondo, M. C., Gil, M., Yela, M., Johnson, B. J., and Ochoa, H. A.: Antarctic ozone variability inside the polar vortex estimated from balloon measurements, Atmos. Chem. Phys., 14, 217–229, , 2014.

Ramanathan, V. and Dickinson, R. E.: The Role of Stratospheric Ozone in the Zonal and Seasonal Radiative Energy Balance of the Earth-Troposphere System, J. Atmos. Sci., 36, 1084–1104, 1979.

Rodgers, C. and Dickinson, R. E.: The radiative heat budget of the troposphere and lower stratosphere, Planetary Circulation Project, Rep, A2, 1967.

Ruiz-Arias, J. A., Dudhia, J., Santos-Alamillos, F. J. and Pozo-Vázquez, D.: Surface clear-sky shortwave radiative closure intercomparisons in the Weather Research and Forecasting model, J. Geophys. Res. Atmos., 118, 9901–9913, doi:http://dx.doi.org/doi:10.1002/jgrd.50778doi:10.1002/jgrd.50778, 2013.

van der A, R. J., Allaart, M. A. F., and Eskes, H. J.: Multi sensor reanalysis of total ozone, Atmos. Chem. Phys.,

10, 11277–11294, doi:http://dx.doi.org/10.5194/acp-10-11277-201010.5194/acp-10-11277-2010, 2010.

WMO: Atmospheric Ozone, Tech. Rep. 16, Global Ozone Research and Monitoring Project, Geneva, 1986.

WMO: Scientific Assessment of Ozone Depletion: 2010, Tech. Rep. 16, Global Ozone Research and Monitoring Project, Geneva, 2011.

Table 1. Description of the ozone profiles in the shortwave schemes in the WRF-ARW model. Dudhia **(SC12R#2)** scheme is ~~and GFDL schemes are~~ not analyzed in this study for the reasons mentioned in the text.
table

Scheme	Profiles	Latitudes	Time	Levels	Location in code
Dudhia	None	–	–	–	–
Goddard	5	3	Summer/Winter	75	Subroutine gsfcswrad in module_ra_gsfcsw.F
New Goddard	5	3	Summer/Winter	75	Subroutine goddardrad in module_ra_goddard.F
GFDL	148	37	4 seasons	81	Subroutine o3clim in module_ra_gfdl.F
RRTMG	1	1	Annual	31	Subroutine o3data in module_ra_rrtmg_lw.F
CAM	768	64	12 months	59	Auxiliary file ozone.formatted
FLG	5	3	Summer/Winter	75	Subroutine o3prof in module_ra_flg.F

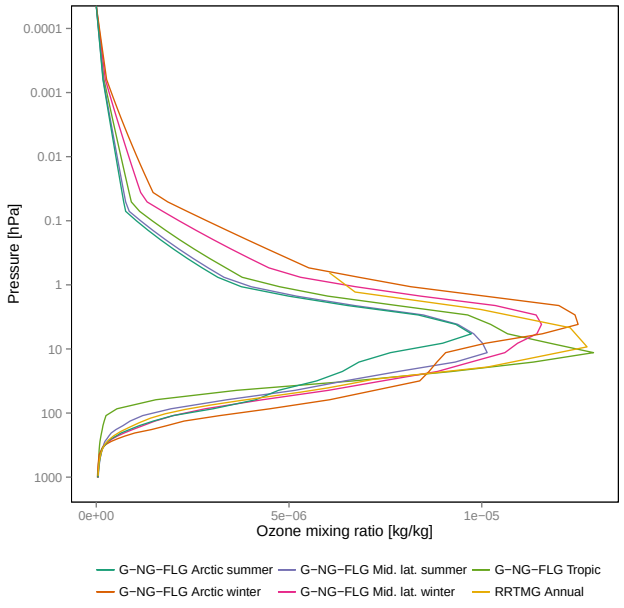

Fig. 1. Ozone profile datasets available ~~Relative error~~ in the ~~total ozone column using the MSR monthly averages for the period (1979–2008) as baseline for RRTMG and~~ G-NG-FLG and RRTMG parameterizations.
figure

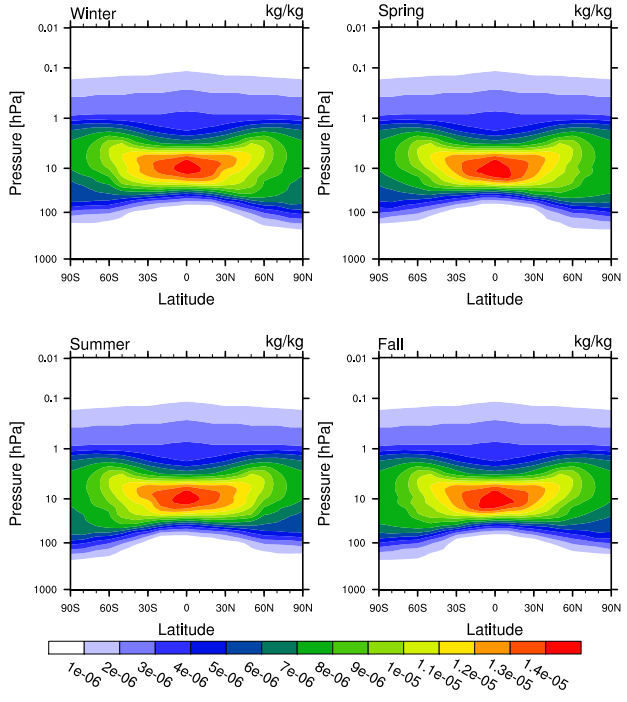

Fig. 2. Ozone profile datasets available ~~Relative error~~ in GFDL~~the total ozone column using the MSR monthly averages for the period (1979–2008) as baseline for CAM~~.

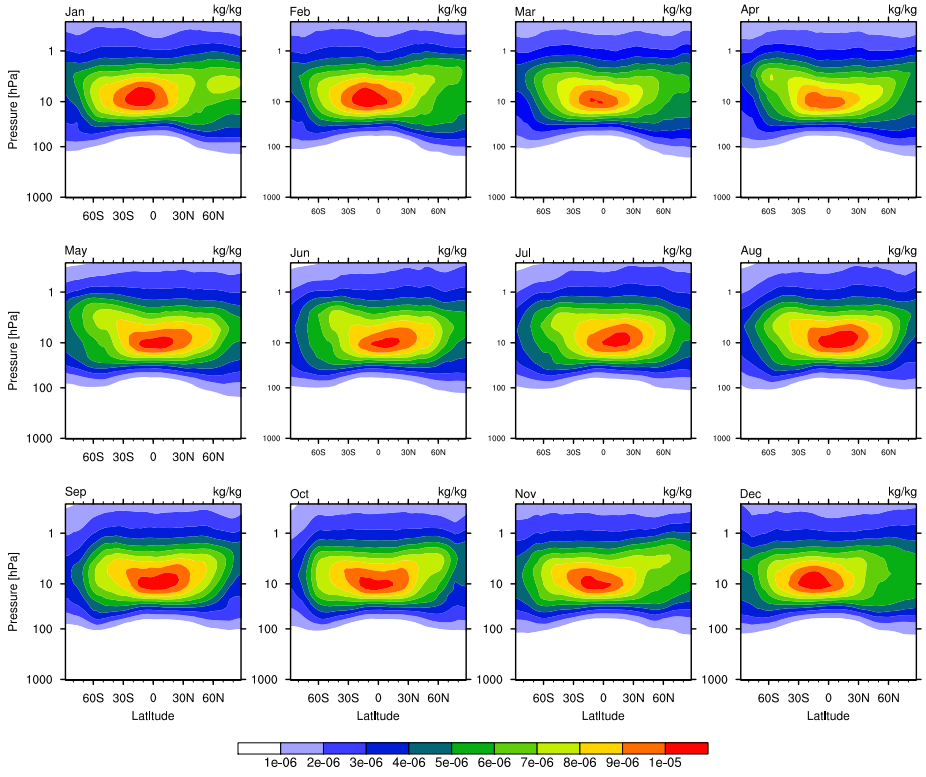

Fig. 3. Ozone profile datasets available ~~Bias~~ in ~~the ozone absorption using the MSR monthly averages for the period (1979–2008) as baseline for New Goddard and~~ CAM.

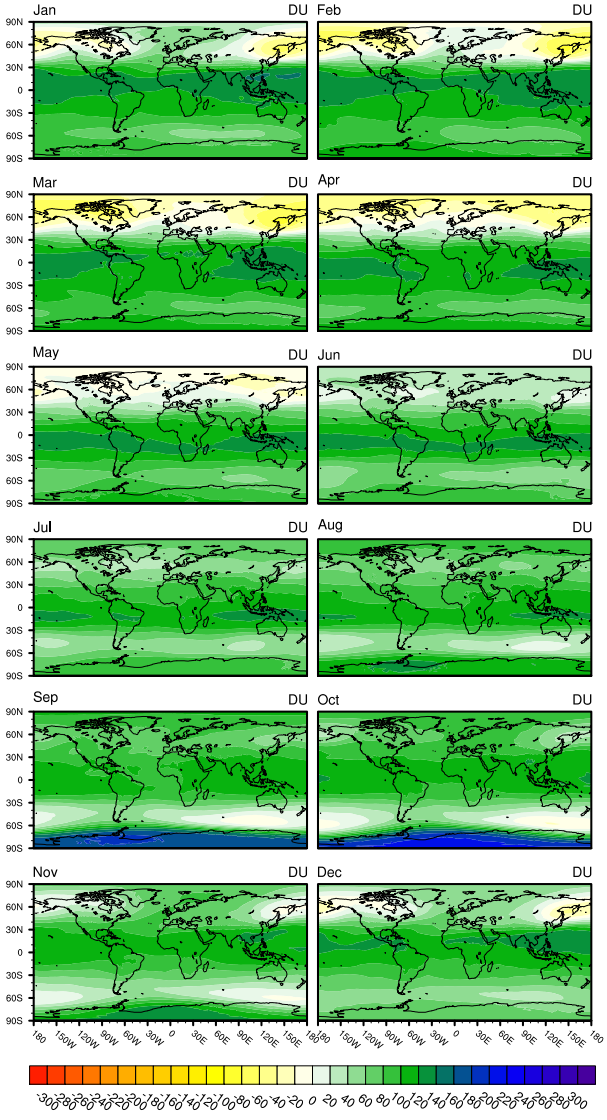

Fig. 4. Bias in the total ozone column using the MSR monthly averages for the period (1979–2008) as baseline for RRTMG.

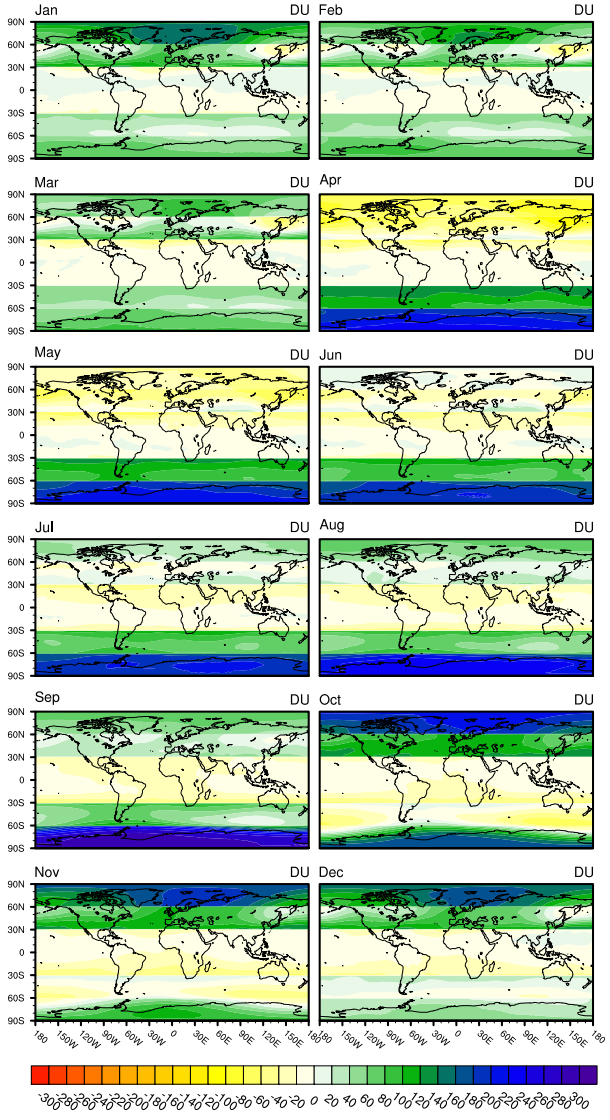

Fig. 5. Bias in the total ozone column using the MSR monthly averages for the period (1979–2008) as baseline for G-NG-FLG.

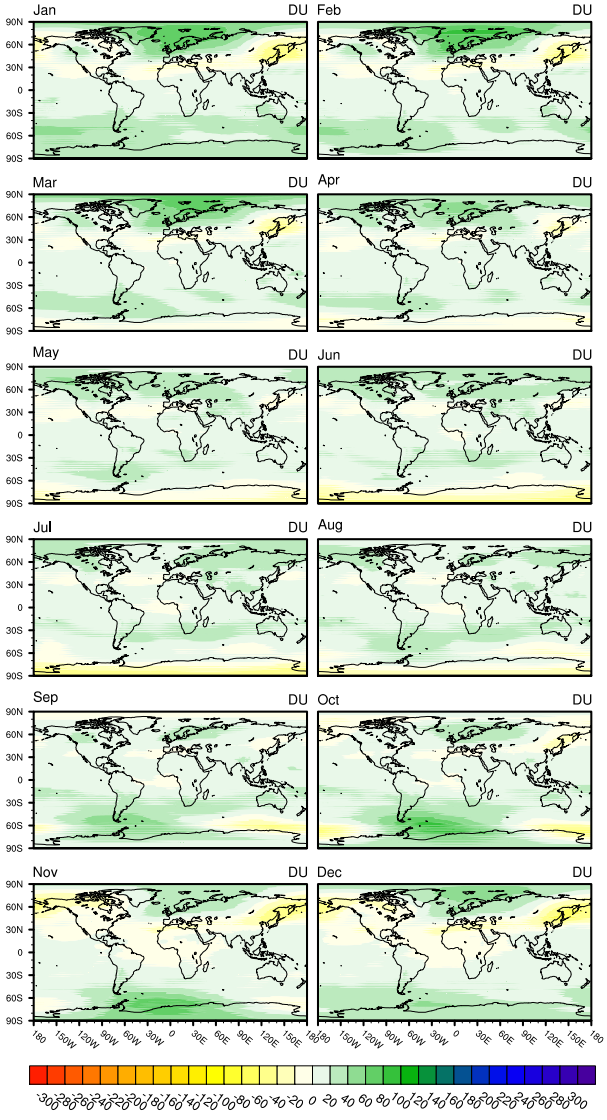

Fig. 6. Bias in the total ozone column using the MSR monthly averages for the period (1979–2008) as baseline for CAM.

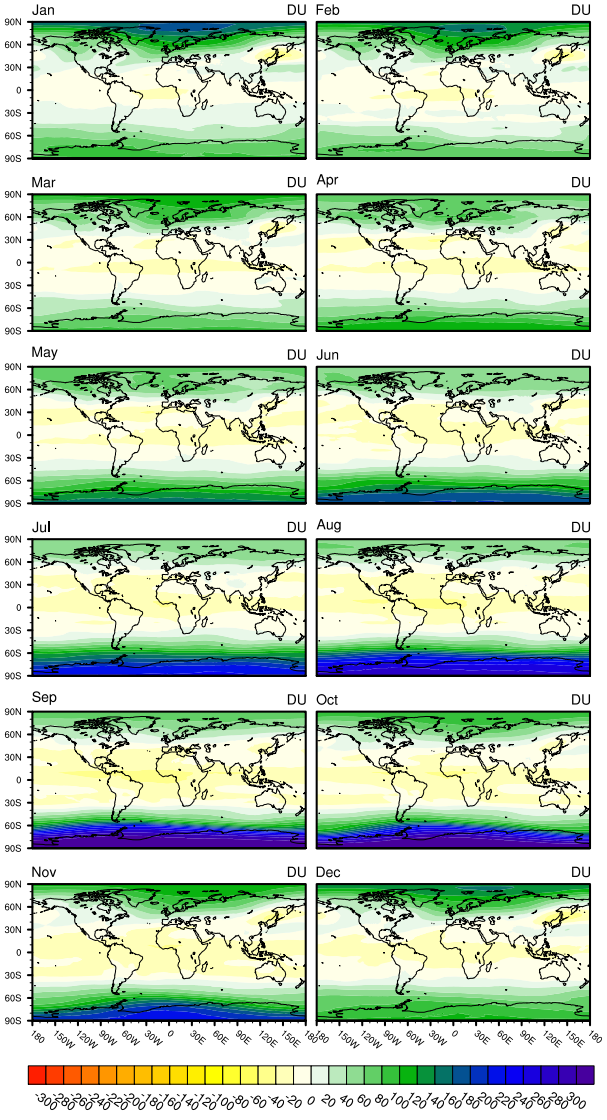

Fig. 7. Bias in the total ozone column using the MSR monthly averages for the period (1979–2008) as baseline for GFDL.

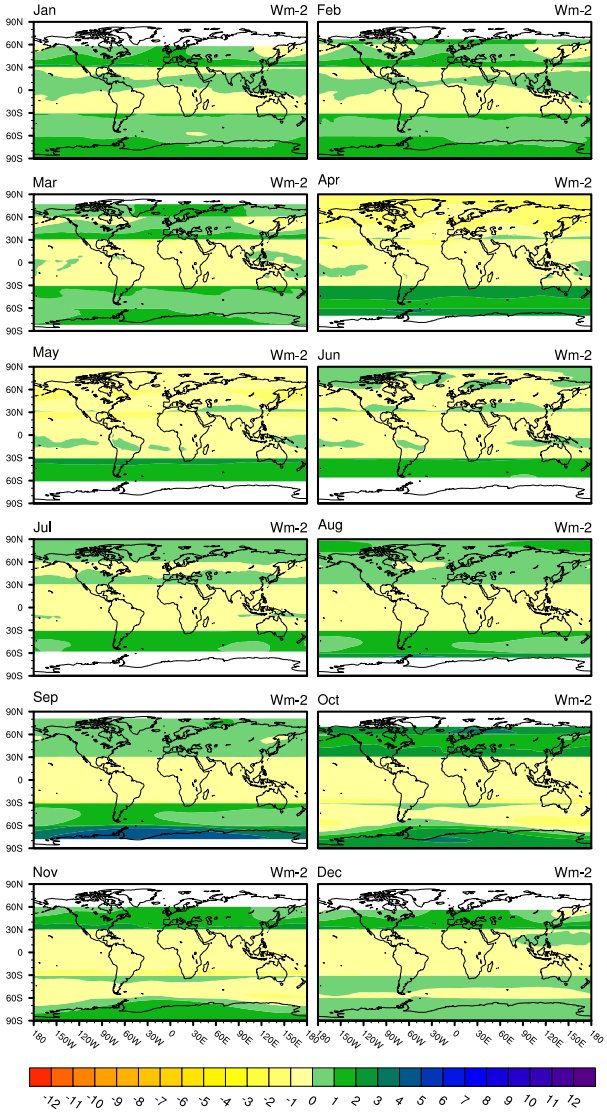

Fig. 8. Bias in the ozone absorption using the MSR monthly averages for the period (1979–2008) as baseline for New Goddard.

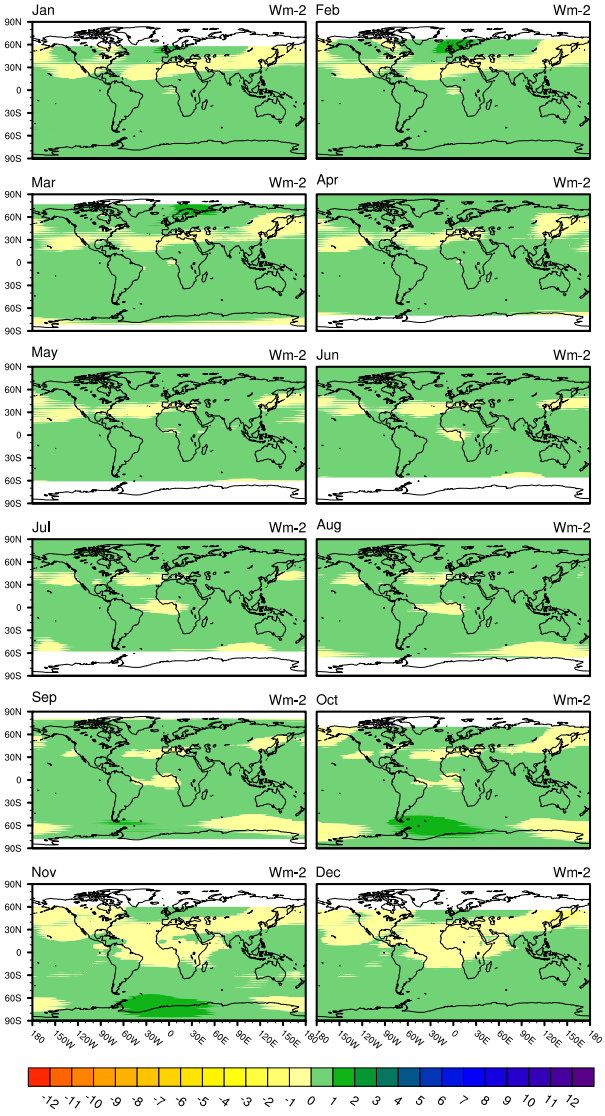

Fig. 9. Bias in the ozone absorption using the MSR monthly averages for the period (1979–2008) as baseline for CAM.

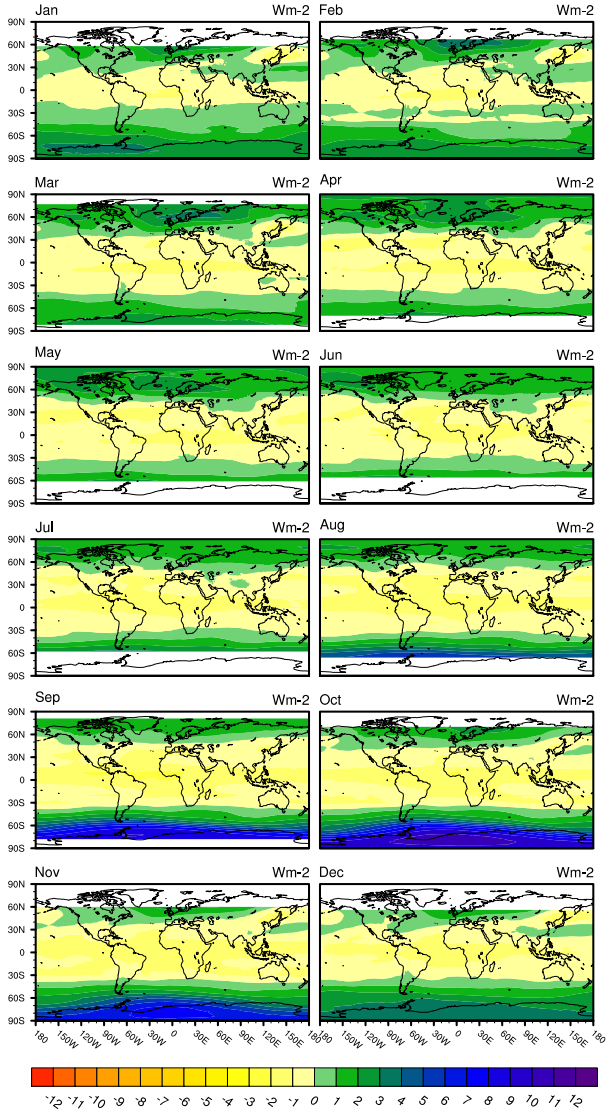

Fig. 10. Bias in the ozone absorption using the MSR monthly averages for the period (1979–2008) as baseline for GFDL.